APPLICATION OF TRAVELLING WIRE-ECSM PROCESS FOR MACHINING OF COMPOSITES

by
P. SREENIVASA RAO

ME
1988 Th
M 620.118
R18a
RAO
APP

Th
ME/1988/M
R189

DEPARTMENT OF MECHANICAL ENGINEERING
INDIAN INSTITUTE OF TECHNOLOGY KANPUR

September, 1988

APPLICATION OF TRAVELLING WIRE-ECSM PROCESS FOR MACHINING OF COMPOSITES

A Thesis Submitted
In Partial Fulfilment of the Requirements
for the Degree of
MASTER OF TECHNOLOGY

by
P. SREENIVASA RAO

to the
DEPARTMENT OF MECHANICAL ENGINEERING
INDIAN INSTITUTE OF TECHNOLOGY KANPUR
September, 1988

20 APR 1989
CENTRAL LIBRARY
I I T. KANPUR
Acc. No. A 104234

Th
620.118
R 18a

ME-1988-M-RAO-APP

CERTIFICATE

This is to certify that the work entitled, "Application of Travelling Wire-ECSM Process for Machining of Composites" by P. Sreenivasa Rao has been carried out under our supervision and has not been submitted elsewhere for the award of a degree.

Dr.V.K. Jain
Assistant Professor
Dept. of Mechanical Engg.
IIT Kanpur

Dr.S.K. Choudhury
Assistant Professor
Department of Mechanical Engineering
Indian Institute of Technology
Kanpur

September, 1988.

ACKNOWLEDGEMENTS

I am deeply indebted to my thesis advisers Dr. V.K. Jain and Dr. S.K. Choudhury, for their valuable guidance throughout the present work. I am greatly benefitted by their advices and suggestions throughout the course of present work.

I express my deep sense of gratitude to Sri V. Raghuram and Smt. Pramela Raghuram for their help, encouragement and hospitality during my stay here.

I am very much thankful to Prof. Prashant Kumar for his valuable suggestions during the course of present work.

I thank Messers R.M. Jha, O.P. Bajaj, B.P. Bhartia, Sarma, Rajesh Aggarwal for their full hearted co-operation throughout the present work.

I should be grateful to my friend Varma for his help throughout my thesis work. I am immensely grateful to my beloved friends Gopalam, Koppaka, Rama Rao, Doji, Madepalli who are responsible for my happy and memorable stay at I.I.T. Kanpur.

Shri S.C. Bharatwal is responsible for the neat tracings of the figures and Shri U.S, Misra for giving the thesis its present form.

Finally, I thank all of my dearest friends who are responsible for my happy and memorable stay at IIT Kanpur

-P.S. Rao

CONTENTS

LIST OF TABLES

LIST OF FIGURES

LIST OF PHOTOGRAPHS

NOMENCLATURE

A	akea of composite laminate (m^2)
d_f	density of fibre (kg/m^3)
d_{fa}	areal density of fabric/mat (kg/m^2)
N	number of CSM/Kevlar fabric layers in laminate
t	thickness of the laminate
MRR	material removal rate (mg/min)
TWR	tool wear rate (mg/min)
WER	wire erosion ratio (%)
TW/ECSM	travelling wire-electrochemical spark machiningg
0_t	average dimetral overcut (mm)
X_1, X_2	factors (or controllable variables), voltage, concentration respectively
Y_u	response
CADEAG-1	computer aided design of experiments and general analysis-1

ABSTRACT

Fibre reinforced composites, though relatively new materials, have already become an important engineering materials. So far the main emphasis of research has been the development of materials, but nowadays more attention is being paid to the industrial production of products made of composites. Conventional machining methods and some un-conventional machining methods like LBM and WJM are associated with many drawbacks. A new approach for the machining of composites using ECSM was successfully applied to the drilling of holes. Achievements in using ECSM for machining composites have stimulated interest in studying and exploring the prospects of wire-cutting by this method. An apparatus for travelling wire-ECSM is designed and fabricated in the laboratory. The results about the feasibility of the process and its performance during machining of composites are presented in this thesis.

The effect of voltage and concentration of the electrol on material removal rate, tool wear rate, wire-erosion ratio and average diametral overcut are discussed. Experiments are carried out on glass-epoxy and Kevlar-epoxy composites, using basic theories of "design of experiments". Analysis is carried out using computer software package, CADEAG-1.

CHAPTER 1

INTRODUCTION AND LITERATURE SURVEY

1.1 Introduction

1.1.1 Composite Materials

A composite material is a materials system composed of a mixture or combination of two or more macroconstituents differing in form and/or material composition and that are essentially insoluble in each other.

Fibre reinforced composites are relatively new materials but they have already become important engineering materials. They are well known for their light weight, high strength, high stiffness and controlled anisotropic properties. Additional advantages that the composites offer over the conventional materials are flexibility in design, corrosion resistance, etc. Today, fibre composites have found such diverse applications as space vehicles, aircraft, offshore structures, automobiles, protective armours, containers, corrosion resistance coatings, sporting goods and electronics. The most widely used fibrous composites are glass-, graphite-, Kevlar-, boron-, and alumina-fibre composites. Plastics such as epoxy, polyester, etc. are the commonly used matrix materials.

1.2 Machining of Composites

So far, the main emphasis of research has been on the development of materials, but nowadays more attention is being paid to the industrial production of products made

of FRP (Fibre reinforced plastics). In aerospace and shipping industries, which are almost classic fields of application, the production of single part is common. But in automotive, machine tool and sporting goods industries, where mass production predominates, the necessity of fully automated and economic production methods arises. The substitution of metals by plastics with glass, carbon or aramid fibre reinforcement does not only require change in design philosophy, but also affects both the particular production technique and the complete production cycle.

The machining of FRP differs in many respects from metal ~~working~~ machining. The material behaviour not only is inhomogeneous, but also dependent on fibre and matrix properties, fibre orientation and the type of weave. Therefore, the machining of FRP requires special demands for the geometry of the tool and its abrasive resistance.

For the machining of glass- and carbon-fibre composites, a conventional tool geometry similar to the one used in metal cutting is usable. Since high abrasion resistance of tool material is necessary while machining these composites, high speed steel (HSS) is unsuitable as a tool material, But, tungston carbide (WC) tools may be used.

In machining of aramid fibre reinforced plastics (AFRP), standard tools are not applicable without severe work material damage like delamination or fuzzing (as shown in photograph No. 1.1). Aramid fibres requires very sharp cutting edges and a tool geometry which inhibits the fibre displacement in front of the cutting edge. HSS tools usually achieve insufficient tool life even in AFRP. In general, the tool life may be increased by coating HSS or carbide with Tin [1] . In some cases, however, the increase of cutting edge radious due to coating may result in a complete failure of tool performance. Moreover, grinding tools which usually possess a negative rake angle are not suitable for the machining of AFRP. Even more difficulties are encountered when the composite material consists of aramid fibres in addition to glass or carbon fibres, because all the requirements of different types of fibres may not be met at the same time. Also, the increasing use of graphite-epoxy composites for the structural frames of an aircraft has posed a new challenge to the drilling operation [2]. Firstly, such materials are very tough, having a high modulus, high strength and a very high stiffness per unit weight. Secondly, improper drilling causes the delamination of the graphite fibres which reflects in the poor quality of the hole. The quality of the drilled hole deteriorates with increasing use of the drill and this can be critical

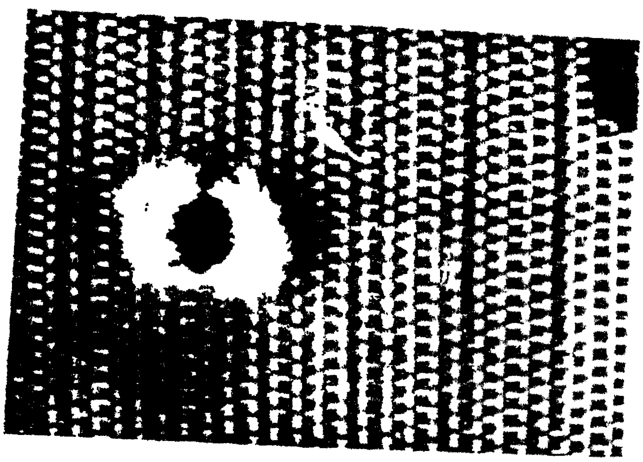

Photograph No. 1.1 Conventional Drilling of Kevlar-Epoxy Composite

to the life of the riveted joints for which the holes are used.

Another serious problem of ~~PRP~~ FRP machining is the generation of airborne dust. Glass and carbon fibre compounds usually emit a fine powder like dust, whereas a fibrous dust is typical for the machining of aramid. In any case, the dust has to be extracted and filtered carefully, since otherwise serious hazards to health and machine tool damage may occur [1].

In view of these facts, the need for developing a new technique for machining of composites, that overcomes the present drawbacks, can not be overemphasised.

1.3 Electrochemical Spark Machining (ECSM)

An advantage of ECSM is that it can be used for the machining of any electrically non-conducting material [3] irrespective of its mechanical properties such as strength, toughness, hardness etc. The geometrical arrangement of the fibers, their weave and their bonding to the matrix are of less importance for the ECSM process. Therefore, the process is ideally suited for the machining of composites.

1.4 Literature Survey

No literature could be forward on "ECSM of composite materials", while limited literature is available on ECSM

process as such [3,7,10,11]. Almost all the processes, that are in use at present, for machining of composite materials have been dealt within [1] and [4] along with their relative merits and demerits.

The different techniques and processes identified with composite manufacturing are as follows:

- methods of cutting cured and uncured composites
- machining technology for routing, trimming, beveling, countersinking and counterboring
- drilling technology
- mechanical fastening
- joining technology, which includes welding, adhesive bonding, brooming and diffusion welding.
- coatings, e.g., paint and special coatings for protection against lighting and electromagnetic interference.

Schwartz [4] gives an interesting analysis of the conventional drilling in composites. In a conventional drill, the neutral rake scrapes the material and causes it to resist penetration by the drill tip. It also tends to push the reinforcing fibers out in front, requiring a great deal of pressure to penetrate in the workpiece. This pressure causes the fibres to bend, resulting in furry and undersized holes. The pressure also produces excessive heat, which causes falling and chip clogging in the resin. The release of pressure as the tool bit breaks through the part causes a sudden and momentary increase

in feed rate. As the tool plunges through the last few fibers, the cutter shaft, not the cutting edge, removes the remaining material. This results in chipping and cracking. The best way to analyse a drilling operation is to examine the chips. If the speed of the cutting tool is too high, heat will make the resin sticky and produce a lumpy chip; if the cutting edge is scraping and not cutting the plastic, the chips will be large and flaky. Either type will eventually clog any evacuation system.

The main problem of drilling FRP is the quality achieved at the tool exit side [1]. Therefore, the width of the damaged zone on that side and the surface roughness have been taken as the best indicators for the drilling result. The quality and the variation of measured values have been shown to be highly dependent on fibre orientation. Also the forces for the drilling of carbon-HT composites are found to be higher than for E-glass reinforcement, as long as the laminate structure is comparable [1]. In order to drill AFRP's orderly the fibres should be preloaded by tensile stress and cut in a shearing motion. It is therefore necessary to pull the fibres from the outer tool periphery towards the centre of the material. This requirement can be met by tools with protruding peripheral cutting edges and positive radial and axial rake angles [1].

For trim routing glass- and carbon fibre compounds tools with multiple cutting edges made of cemented carbide, or polycrystalline cutting materials are recommended [1]. The best machining quality is achieved by upmilling, independent of tool geometry and cutting conditions. Similar to drilling, the amount of cutting force and the surface quality in routing is very much dependent on fibre orientation.

Conventional routing tools with oxidational twisted helix are not suited for the routing of AFRP because fuzzing occurs due to axial cutting forces at the top layer which is not backed by adjacent material layers [5]. A straight flute design achieves a high machining quality at first, but after a very short cutting path rapidly increasing fuzzing occurs at both top layers [5].

Circular ~~showing~~ Sawing uses diamond blades for most composite materials [4]. Cutting speed for composite normally varies from 2000 to 10,000 ft/min. Thicker parts ar cut at proportionally lower feed rates. Saber sawing normally cuts Kevlar-epoxy with a blade which cuts the outermost on both sides of the laminate towards the interior. Blade speeds of 2500 strokes ~~free~~ per minute are recommended, but blade speed and feed rates may vary with material thickness.

Reciprocating-knife cutting is another technique used for the cutting of composites. There are two types of systems, both of which incorporate high-speed ~~reciprocatin cating~~ Recipro knives that are driven through the material to be cut by a mini-computer controlled, XYZC positioning system. In one system the cutting knife penetrates through the material into closely packed plastic bristles that constitute the surface of the cutting table. The system cuts in chopping mode, i.e., the knife rises above and plunges through the material onto the table. The second system can cut desired patterns in a continuous line at high speed. Curves, sharp corners, and notches can also be cut without lifting the knife from the material. Cutting results for both system indicate that the slicing and choping system can cut a greater number of glass-epoxy and graphite-epoxy plies at twice the feed rate of the choping system.

A widely used technique for the machining of FRP is Water Jet Cutting (WJC) [6]. From the physical point of view, the water jet has good preconditions for cutting FRP. Especially thermal material damage is completely avoided. For contour cutting operations, which are very common in FRP machining, the almost point sized "tool" geometry and the multidirectional cutting ability of WJC are favourable.

Inspite of these advantages, WJC has two major drawbacks [1]:

(1) Perpendicular to its own axis the jet has only limited stability and may therefore easily be distorted within the cutting kerf. Due to this the cutting front, which is visible at the cut surface as a bundle of parallel grooves, is bent opposed to the feed direction. If the jet hits an obstacle, for example a fibre embedded in matrix, it will be deflected and will erode the "soft" components of the material first. Therefore FRP surfaces cut by water jet show that typical appearance of "washed out" matrix and protruding fibres. At the cutting limit the jet will erode matrix material only and will "jump" clearly visible and audible across the fibres, which remain as solid links across the kerf.

(2) The jet force acts in the direction of the fluid flow and therefore generally perpendicular to the surface. This force direction, however, as pointed out earlier, is mainly responsible for material damage at the tool exit side.

Additionally, the cutting process at the bottom of the Kerf is slowed down due to the fact, that power density and therefore penetration ability has been absorbed by the layers above. This results in cracking and chipping at the exit side. The feed rate attainable is therefore in general limited by the surface quality required ~~routes~~ rather than the rough cutting ability of the jet.

Next to WJC the laser cutting technique is well suited for the contour trimming of FRP [1]. In general, aramid fibres are well, glass fibres less and carbon fibres hardly suited for laser cutting. This technique requires very precise control of focus position, feed rate and process gas flow. Especially this later parameter is, next to the power density and the intensity profile, the most important factor for the thermal damage of the material. Thermal damage is one major drawback of the laser technique besides the generation of smoke and fume. Surface quality and kerf geometry especially for thin laminates are very good, if single mode laser are used [1].

1.4.1 ECSM Process

In this process, two electrodes, one of which is the tool of the desired shape, and the other a flat plate of much larger area than the tool, are immersed in an electrolyte with a certain distance ($\sim$30-50 mm) maintained between them. It has been observed that the sparking occurs at the tool electrolyte interface above a certain voltage (30-60 volts). This sparking is not between electrodes, but from the tool to the electrolyte, presumably across a hydrogen or steam layer. Now if the sparking tool is brought in contact with the workpiece, which is kept between the two electrodes, machining takes place.

Cook, Foot, Jordon and Kalyani [3] have studied the discharge machining of glass. The process is shown to be electrolyte sensitive, and also varies somewhat with polarity. Further, for a given voltage, the rate of machining decreases with time. Machining rate increases both with concentration and temperature of electrolyte. Machining occurs more readily at corners. A pulsed d-c voltage supply was also used to test the effect of high frequency pulsed current [3] . It is found that for pulsed power supply (pulses in milli-sec range), the material removal rate is comparable to the case when d.c. power is used. For pulses in the micro-sec range, MRR increases by a factor of two. More striking is the effect of pulsed power (milli-sec or micro-sec) on the surface finish of the holes. The surface produced by pulsed power is found to be much smoother than that from a d.c. power supply. A variety of electrically non-conducting materials have been machined successfully using ECDM. Some of the results obtained by Cook et al. [3] have been confirmed by Kumar [7].

A special mention needs to be made about the sparking in ECM. Larsson and Baxter [8] discussed about the reasons for sparking in ECM. For sparking to occur, metal-to-metal contact does not seem to be necessary. The onset of sparking coincides with the formation of large flat bubbles. Such bubbles are blanketed a much larger area of the electrode than the more spherical bubbles. The sparking between the

electrode and the electrolyte solution could be clearly seen if two wire electrodes are held just touching onto the surface of static electrolyte with a voltage of 100 volts or more. Violent sparks can be produced particularly at the cathode, although potential gradient is probably more important than the potential difference. In an ECM cell, if the cathode becomes covered with a layer of thin large area bubbles, the current will be conducted by streamers of electrolyte between the bubbles thus causing a high potential gradient. Larson, et al [8] also reported that the sparks observed per square mm of tool could be an inverse function of the gap, and the number of sparks decreases after some time as the process proceeds. According to Loutrel and Cook [9], fields in the order of 10^6 volts/cm ase generally required to produce field emission arcs in dielectrics. For the case of the electrolyte found in ECM, they theorize that arcs always form across voids. If the voltage gradient across the void exceeds the dielectric strength or break down voltage, an arc will occur. Once an arc is initiated, it may eihher die or grow larger. After an arc is initiated, the heat produced will begin to vaporize the surrounding electrolyte causing the void to grow larger. If the voltage gradient in the surrounding electrolyte is high, as in extreme machining conditions, the arc will continue to grow, bridging the gap and causing melting of the electrode surfaces. This is a typical failure point in

ECM. Loutreal et al. [8] have suggested the following seven mechanisms leading to high voltage gradients in the presence of voids :

(1) Electrolytic gas evolution at electrode surfaces
(2) Depletion layers
(3) Electrode passivation and activation over voltages
(4) Local stagnation of flow
(5) Steam generation and cavitation
(6) Vapour blanketing of electrode surface
(7) Particles in electrolyte flow.

Khouyry and McGeougw [10] have discussed metal removal in the leading and side. Gaps of ECDM drilling (for a conducting workpiece). Electrochemical dissolution (ECD) and electrodischarge erosion (EDE) are shown to occur as discrete phases of round only varying intensity and duration. The random occurrance of spikes in both working voltage and machining power that arise during the ECD and EDE phases is described in terms of stochastic difference equations which are obtained from the dynamic data systems (DDS) modelling method. The special moments of the voltage and profiles developed from these models are used to discriminate between the phases of ECD, and the occurrence of arcs and sparks in machining gap. The analysis of machining power is shown to

to be useful only for qualitative assessments.

Crichton and McGeough [11] have used high speed photography to show that both spark and arc discharges are possible in an electrolyte. Further it is shown that the type of discharge may be distinguished from the energy of emitted radio frequencies or by the study of the light emitted. According to them, on application of a voltage pulse between two electrodes immersed in an electrolyte, three phenomena may occur: (a) Electrochemical action only, (b) electrochemical action followed by discharge between an electrode and the electrolyte, and (c) electrochemical action followed by discharge between the electrodes. Within the single pulse voltage and current waveforms obtained with phenomenon (c), four electrical stages may be distinguished:

(1) high frequency oscillation (170 KHz),

(2) high rate ECM,

(3) low rate ECM, and

(4) electrical discharge.

Stage 1 represents an unproductiwe period, however further work by the authors [11] has shown that it may be eliminated by circuit modification. Stage-2 and 3 together represent an ECM phase, and stage-4 an EDM phase. The duration of these phases respectively increase and decrease with increasing gap width and vary with electrolyte type, concentration and conductivity.

A comparison of ECDM with USM (ultrasonic machining) has been made by Kumar [7] . ECDM is reported to be having some distinct adaantages over USM. The initial investment required for USM would be larger than that required for ECDM. The penetration rate of 2 mm/min obtained in ECDM is faster than the 1.5 mm/min obtained in USM (using stainless steel circular tool of 1.6 mm diameter). Moreover the surface roughness of about 0.3 microns obtained with ECDM is also smaller than 0.5 microns obtained with USM (for a glas workpiece). Also it is found that with a rectangular tool the corners are less rounded with ECDM.

ECDM has been successfully applied to hole drilling in composites by Tandon [12] . Effect of voltage, electrolyte conductivity, fiber volume fraction and tool diameter on material removal rate, tool wear rate (TWR) relative tool wear and overcut were studied by him.

He reported, increase of MRR, TWR and overcut with increase in voltage and electrolyte conductivity and with decrease in tool diameter. Fibre volume fraction was reported to have no effect on TWR and overcut and slight decrease in MRR with increase in fibre volume fraction. Optimal MRR and TWR for given overcut were also reported.

1.5 Objectives of Present Work

From the above literature survey it is evident that am efficient and accurate technique for machining of composit

is not available. Conventional machining methods are associated with many drawbacks, while laser cutting, apart from being inefficient, gives large heat effected zone. Water jet cutting, besides being expensive has limited applications. But, ECSM in which material removal rate is independent of mechanical properties of composites, seems to be a potential process for machining of composite materia

ECSM has been applied 12 to drill holes in the composite materials. Achievements in using ECSM for machining composites have stimulated interest in studying the prospects of travelling wire-electrochemical spark machining (TW/ECSM), especially in the light of rapidly growing industrial use of composites. The main advantages invisaged for ECSM with a wire electrode [13,14] are:

1. Cutting of large volumes of material, without the need for costly full-form tool electrodes, or for large power supplies.
2. By numerical control of the direction of movement of the workpiece, complex two/and three/dimensional shapes in the workpiece can be produced.

At present stage, no data is available concerning the effects of TW/ECSM on MRR and overcut etc. when machinir composite materials. To gather relevant information, an apparatus for wire ECSM was designed and fabricated in the laboratory. The feasibility of machining composite material

using this apparatus was studied. Glass-epoxy and Kevlar-epoxy laminates were used as work material.

Voltage, concentration were taken as independent parameters. Their effects on material removal rate (MRR), tool wear rate (TWR), wire-erosion ratio (WER), and overcut produced was studied.

is not available. Conventional machining methods are associated with many drawbacks, while laser cutting, apart from being inefficient, gives large heat effected zone. Water jer cutting, besides being expensive has limited applications. But, ECSM in which material removal rate is independent of mechanical properties of composites, seems to be a potential process for machining of composite materials.

ECSM has been applied [12] to drill holes in the composite materials. Achievements in using ECSM for machining composites have stimulated interes t in studying the prospects of travelling wire-electrochemical spark machining material removal rate (MRR), tool wear rate (TWR), wire-erosion ratio (WER), and overcut produced was studied.

CHAPTER 2

EXPERIMENTATION

2.1 Experimental Setup

Figure 2.1 shows a schematic diagram of the experimental apparatus. The experimental set-up consists of an electric power source, gravity type feed mechanism, a wire-feeding system, two electrodes and a tank of electrolyte.

The electric power source consists of a variac to control the voltage supply to the system and a bridge rectifier consisting of four diodes to supply the d.c. power.

Gravity feed was provided to the workpiece. Gravity type feed mechanism consists of an adjustable work support, pulley, pan and a counter weight. The feed forceøon the workpiece can be adjusted by adjusting the counter weight. By this feed mechanism, workpiece and wire are always in physical contact with each other.

The main components of the wire driving system are shown in Fig. 2.2. It consists of a frame, two wire guides (pulleys), one double groove pulley, two spools (feeding and take-up spools), d.c. stopper motor and its controller.

Initially, copper was used for the flat electrode as anode. But due to the electrolytic action, copper was getting dissolved resulting in a large amount of sludge and contaminating the solution, on the other hand, graphite which does not

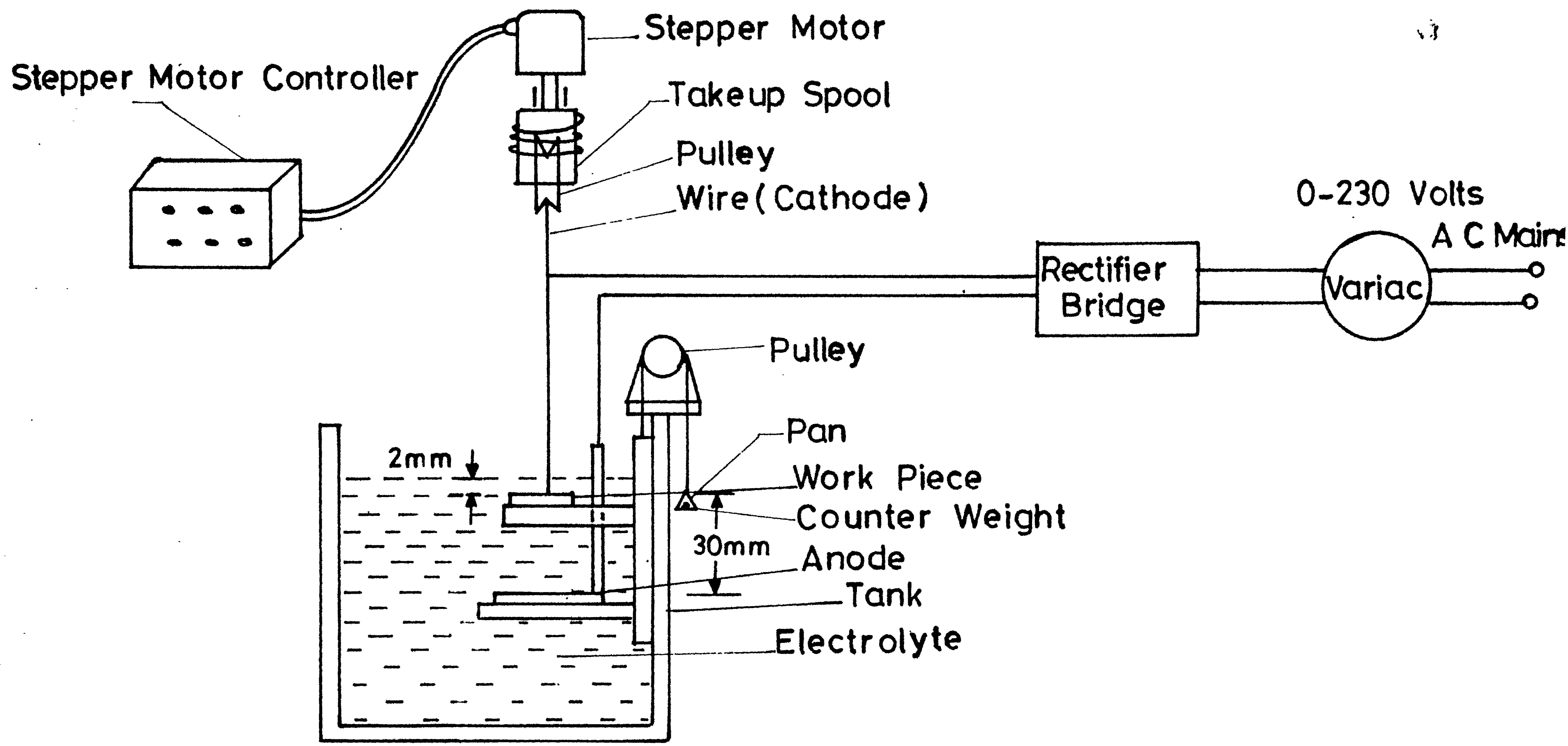

Fig. 21 Schematic Diagram of TW/ E C S M Process.

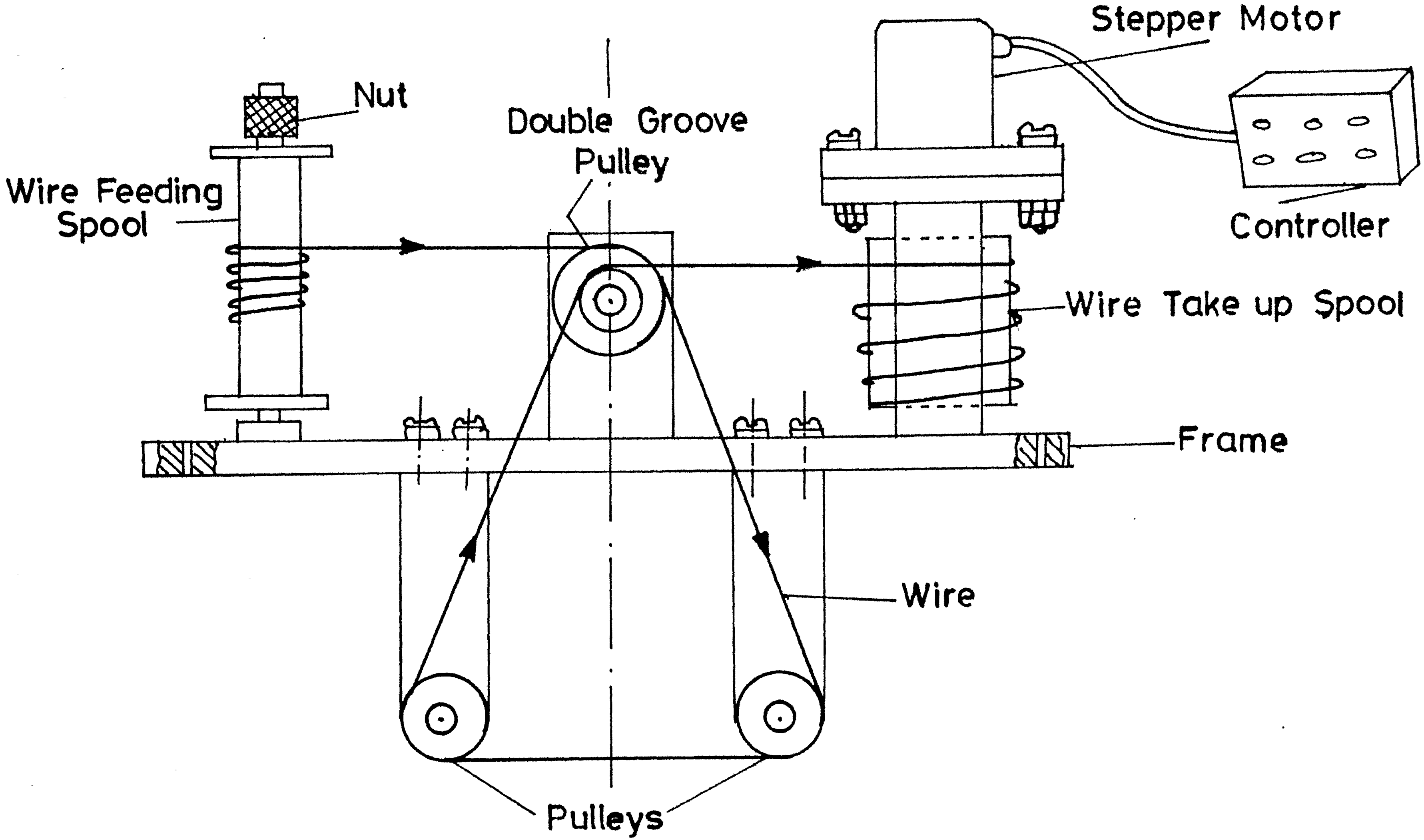

Fig. 2.2 Wire-Feeding System.

form the sludge did not contaminate the solution. In view of this, graphite plate of 9.5 mm x 7.5 mm x 1.0 mm was used as anode when brass wire of 0.6 mm diameter was used as cathode, the wire was breaking quite frequently because of its low current carrying capacity. After its use for some time in the process, it used to get red hot and finally broke even at 55 volts. For achieving some realistic MRR, voltage higher than 55V is required. Hence copper wire of 0.922 mm dia was used in all the experiments. Current supply to the wire was given through a double groove pulley. Wire is driven at a constant speed of 12 mm/min. using a stepper motor.

In the beginning, the experiments were conducted with aqueous solution NaCl as electrolyte. But MRR achieved was very low. Electrolyte flushing was also tried with NaCl to remove the debries from the tool-work interface. The flowing electrolyte tests could not yield successful results since the flowing electrolyte carried away the gas bubbles, thereby reducing the sparking and hence the machining. To increase the MRR, NaOH was tried. Since NaOH has a higher specific conductance even at lower concentrations, higher rates of reaction takes place, so larger amount of gases are evolved in case of NaOH. Hence higher MRR was observed. For this reason, all the experiments reported in this thesis, were carried out with NaOH. Specific conductance of NaCl and NaOH solutions at various concentrations [15,16] are given in the Table 2.1 and figure 2.3.

Workpieces used were of glass-epoxy and Kevlar-epoxy composites of size 7.0 mm x 2.5 mm x 3.0 mm. Gl-ep and KV-ep composites were found to have the fibre volume fractions as 45% and 44% respectively. Workpiece is held at a ~~distance~~ distance ~~distance~~ of about 30 mm from the anode. Wire was kept in contact with the workpiece which was fixed at about 2-3 mm below the level of the electrolyte.

An overall view of the apparatus is shown in Photograph No. 2.1 and wire-feeding mechanism is shown in Photograph No. 2.2

2.2 Specimen Preparation

The present investigations have been performed on Kevlar-49 fabric reinforced epoxy resin. Kevlar-49 fabric specifications supplied by the manufacturer are given in Table 2.2. This fabric has the fibre volume ratio in warp and fill direction as 10 :1. This type of weaving is generally referred to as the unidirectional weave.

The specifications of the epoxy supplied by the manufacturer are given in Table 2.3. Curing temperature and corresponding curing times as suggested by the manufacturer are given in Table 2.4.

Composite plates of 3 mm thickness were cast by hand lay-up technique in the laboratory. Fabric was cut into the required size by a special Kevlar cutting scissors, supplied

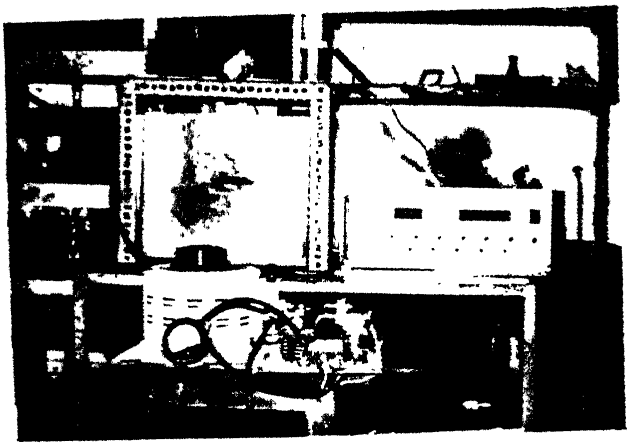

Photograph No. 2.1 An Overall View of TW/ECSM Apparatus

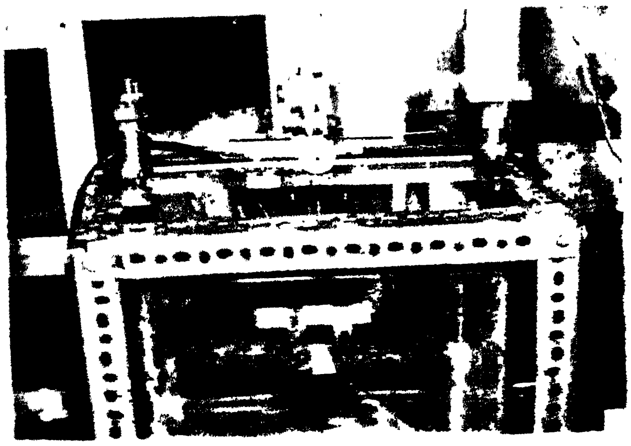

Photograph No. 2.2 Wire-feeding System

by fabric manufacturer (Dupont Company). To obtain maximum fiber volume fraction along with good surface finish, ten layers of fabric were used for 3 mm thick laminate. Fabric was demoisturized completely by pretreating it in an oven at 105^{o}C for 16 hours. It was then cooled in the oven itself so that no moisture could be absorbed again.

Composite laminates were cast between 25 mm thick mild steel mould plates lined with mylar sheets. These sheets make it easy to release the laminate from plates and also ensure a good surface finish. The fabric pieces were placed on the lower mould plate one by one. Resin was spread by a brush, on lower mould plate and on the top of each fabric piece. The laminate was rolled gently with a rubber roller.after placing mylar sheet on the top. Rolling squeezes out the entrapped air and the extra epoxy. The upper mould plate was then placed on the top. The mould plates were separated by mild steel spacers to control the thickness of the laminate. The mould plate applies a pressure due to its own weight and due to tightening of nuts on the bolts, going through both the mould plates. Excess resin gets squeezed out from the sides.

The plates were cured at room temperature for about 6 hours and then at 55-60^{o}C for another 12 hours by heating the mould plates through several 250w heating elements placed
ter surface of each mould plates. The rate of
ould be controlled through a transformer.

Experimental determination of fiber volume fraction for Kevlar fiber composites is not possible, because in the resin burn-off test, the fibers also burn off. Therefore, following indirect method is used [17].

Fiber Volume Fraction :

$$V_f = \frac{AN\rho_{fa}/\rho_f}{A.t} = \frac{N\rho_{fa}}{t\rho_f}$$

where,

A = Area of composite laminate.

N = Number of fabric layer in laminate

= 10

ρ_{fa} = Areal density of fabric

= $0.190\ kg/m^2$

ρ_f ρ_f = Density of fiber

= $1.44 \times 10^3\ kg/m^3$

t = Thickness of laminate

= 0.003 m

Hence,

$$V_f = \frac{10 \times 0.190}{0.003 \times 1.44 \times 10^3}$$

$$= 0.4398\ (\simeq 44\%).$$

Specimens of size 70 mm x 25 mm were cut on a circular sawing machine. Unconventional side of a metal splitting fine teethed H.S.S. cutter was used at high speed ($\sim$30 m/s). The quality of the edge is found to be quite good except few broomed fibers at one side of edge from which cutter is released after cutting. This brooming can be easily removed by ~~sawding~~ Sanding the edges on simple wood sanding paper and a good edge finish is obtained.

Glass-epoxy laminates of 3 mm thickness supplied by 3M company USA were also used. It is a cross-ply $(0/90)_{4S}$ laminate having 16 layers and fiber volume fraction 45%.

Specimens of same size as that of Kevlar-epoxy composites were cut with the help of a diamond cutter.

2.3 Experimental Procedure

Experiments performed on glass-epoxy as well as on Kevlar-epoxy composites were planned according to the "design of experiments" technique [18,19] . Voltage and concentration were considered as controllable variables and their effects on material removal rate (MRR), diametral average overcut, tool wear rate (TWR) and wire-errosion ratio (WER) were studied as responses of the process. Table 2.5 gives the levels and their actual values for different factors.

Table 2.5

Values of X_1 and X_2 for Different Levels

		Levels				
Factors	Symbol	-2	-1	0	1	2
Voltage (volts)	X_1	55	60	65	70	75
Concentration (grams/litre)	X_2	5	10	15	20	25

The scheme of experimentation and responses obtained are given in Appendix A.

Each experiment was carried out till the minimum depth of penetration of the wire in the workpiece is equal to the diameter of the wire. Machining was stopped after every minute to monitor the specific conductance of the electrolyte which increased due to the temperature rise. It was brought back near to its original value by allowing the electrolyte to cool down to approximately room temperature by stirring the electrolyte and using a fan. Electrolyte was filtered after each experiment to remove the sludge from it. Fresh electrolyte was used for every new trial.

Experiments were performed for a duration of time ranging from 2 to 35 min. for glass-epoxy composite and 7 to 35 min. for Kevlar-epoxy composite. During experimentation, current was recorded from the ammeter at every half minute interval. History of current variation during ECSM is shown in Fig. 2.4. After machining, both the wire and workpiece were cleaned and reweighted, with the help of a single pan microbalance (accuracy of 0.00001 gm). The amount by which the width of the machined slot exceeds the wire diameter, i.e. the "diametral overcut" illustrated in Fig. 2.5 was measured with the help of a shadow graph taken at a magnification of 20X. Some of the shadow graphs showing overcuts are given in Appendix B.

The wire erosion, defined as the ratio of weight loss of wire to that of the workpiece was also calculated. Wire-speed was estimated from the product of the circumferential diameter of the spool including wire and the rate of revolution.

The responses thus obtained were fed to a computer programme CADEAG-1 [20] to get the relationship between different parameters and responses. Additional experiments, Table 2.7 and Table 2.9, Appendix A, were performed to check the validity of the model.

2.4 Process Modelling

It is difficult to formulate a simple mathematical model for the complex process such as travelling wire ECSM.

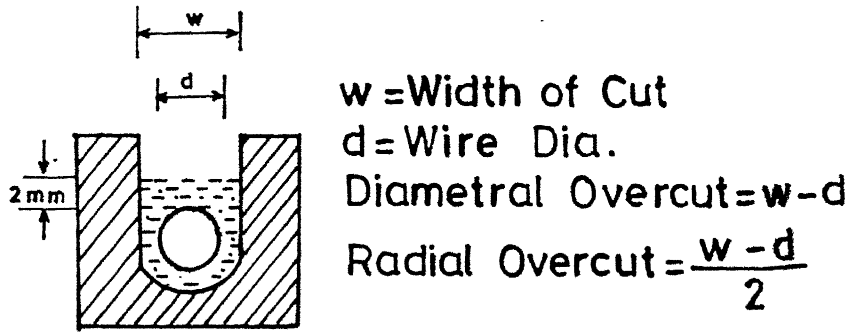

Fig. 2.5 Overcut Generated During the Machining Process with Wire.

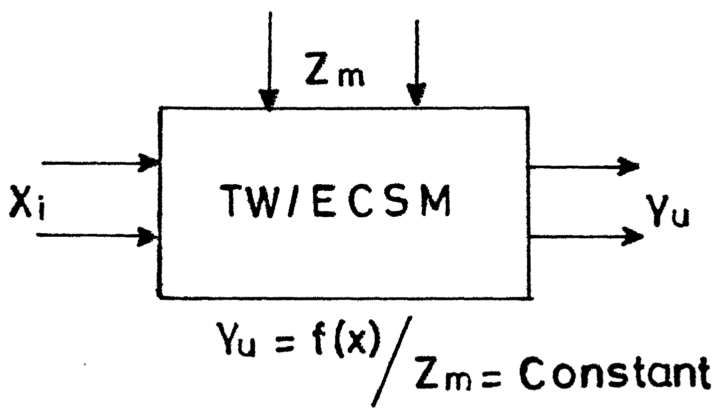

Fig 2.6 A Model of the TW/ECSM Process.

However, the wire ECSM process may be modelled as a block box system where investigations into the effect of electrolyte concentration and voltage on output quantities can be based on the model shown in Fig. 2.6

In this figure X_i are the factors, effects of which on the process have to be investigated. Z_m are the factors held constant during the test and Y_u are the measured values of the responses. In the present study, X_i are defined as: electrolyte concentration and voltage; Factors Z_m are identified as: type of electrolyte (NaOH), wire material (copper), wire diameter (0.922 mm), workpiece material (Glass-epoxy/ Kevàar-epoxy composites); and responses Y_u are identified as: material removal rate (mg/min), diametral average overcut (mm), tool wear rate (mg/min), and wire-erosion ratio.

2.5 Design of Experiments

The experimental work carried out to study the effects, is planned in accordance with the statistical techniques of the experimental design. According to Adler, Markova and Granvosky [19] the design of an experiment is the procedure for selecting the number of trials and conditions for running the experiments, essential and sufficient for solving the problem that has been set with the required precision. The important features are as follows:

(a) The simultaneous variation of all the variables determining a process according to special rules called algorithms;

(b) Striving to minimize the total number of trials and,

(c) The selection of a clearcut strategy permitting the experimentor to make substantial decisions after each series of experiments.

With a well designed experiment it is possible to determine accurately, with much less effort, the effect of change in any one variable on the process output (also known as response or yield) and the interaction effects between the different factors if any. If all the investigated factors are quantitative in nature, then it is possible to approximate the response Y_u as a polynomial equation 1.

$$Y_u = b_o + \sum_{i=1}^{K} b_i x_i + \sum_{i=1}^{K} b_{ii} x_i^2 + \sum_{i<j} b_{ij} x_i x_j \tag{1}$$

where x_i $(i = 1,2,....K)$ are coded levels of K quantitative variables and b_o, b_1 etc. are the least square estimates of the regression coefficients. The polynomial in equation (1) is also known as regression function and the first term under the summation sign pertains to linear effect, the second term under the summation sign pertains to quadratic

effects, and the third term pertains to interaction effects of the investigated parameters.

The actual values of the levels for the factors, X_1 and X_2 are shown in Table 2.5.

CHAPTER 3

RESULTS AND DISCUSSION

3.1 Mechanism of ECSM Process

As already explained in section 1.4.1, the sparking takes place across the tool-electrolyte interface. It is because of the high potential gradient across the hydrogen gas bubbles (hydrogen gas is evolved due to the electrolytic action). Due to the high potential gradient, breakdown of the gas in the bubbles takes place and a discharge occurs. Discharge is accompanied by a large amount of heat.

Machining takes place, since the sparking tool is in contact with the workpiece. The various possible mechanisms by which the material might have been removed are listed below:

1. Melting and vapourisation of the work material
2. Electrochemical action
3. Mechanical erosion.

Due to sparking, the large amount of heat is generated between the tool and the workpiece, as in EDM. It causes the melting and evaporation of the work material. This is confirmed by the presence of the globules (the solidified material) on the protruding fibres, as shown in the Photograph No. 3.1. Heat effected zone can be seen in Photograph No. 3.2.

Gl-ep composite
Voltage = 65 volts
Concentration = 25%
Magnification = 100X

Photograph No. 3.1 Globules on the Fibre Protrusions

Gl-ep composite
Voltage = 60 volts
Concentration = 20%
Magnification = 50X

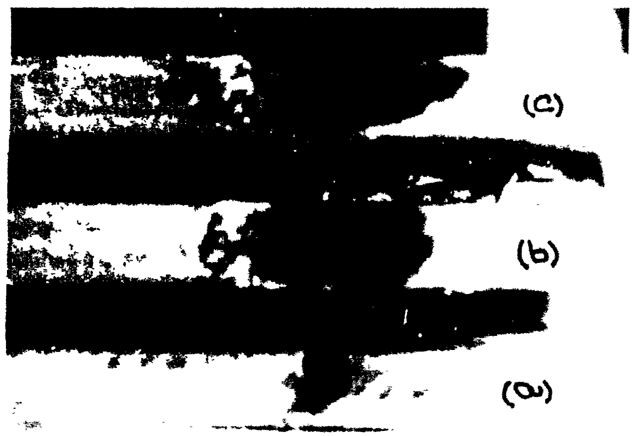

Gl-ep Composite
(a) 65 volts & 15% concentration
(b) 70 volts & 15% concentration
(c) 75 volts & 15% concentration

Kv-ep Composite
(a) 65 volts & 15% concentration
(b) 70 volts & 15% concentration
(c) 75 volts & 15% concentration

Photograph No. 3.2 Heat Effected Zone (HEZ)

It was investigated by Cook [3] and Kumar [7] that the non-conducting materials like granite, Refractory fire-brick, Aluminium oxide, Bakelite, bones and perspex could also be machined by this process. The absence of conducting ions in perspex, granite and refractory brick etc. shows that the material removal by electro-chemical action is not possible.

The third possibility i.e., the mechanical erosion may occur due to the cavitation effect of the gas bubbles rupturing on the workpiece. The discharge through the bubbles will result in its violent rupture.

Material removal by melting and vaporisation seems to be contributing to a greater extent in the machining. However, the mechanism of the process is far from being clear and is apparently quite complex. This should be investigated further.

3.2 Cutting of Glass-Epoxy and Kevlar-Epoxy Composites

Here, the results of travelling wire ECSM of glass-epoxy and Kevlar-epoxy composites are presented. Using the responses, obtained experimentally and given in Table 2.6 and 2.8, Appendix A, response surface model, Eq. 1, was evolved with the help of a computer software package, CADEAG-1. Using these models, effects of different factors (voltage and concentration of electrolyte) on the responses have been studied and are discussed below. In each graph, curves show the computed results, while the points (circle, cross, triangle, square etc.) are the experimental observations.

It is seen that there is a good agreement between the experimental points and the analytical curves derived from the models.

Some of the photographs of the specimens as machined by TW/ECSM are also shown in Photograph Nos. 3.4 and 3.5.

3.2.1 Material Removal Rate (MRR)

MRR is defined as the total material removed from the workpiece divided by machining time.

The effect of voltage on MRR for Gl-Ep and KV-Ep is shown in fig. 3.1.for different concentrations of the electrolyte. MRR is seen to increase with the increase in the voltage. Increase in voltage implies higher discharge energy and hence more MRR.

Microscope observations of the machined pieces have shown micro-cracks at higher applied voltages (70V and above). This may be due to the higher thermal energy input and the subsequent thermal cracking of the glass-epoxy composite. This shows that the material is removed mainly due to thermo-mechanical effects. Cracks can be seen in Photograph No. 3.3.

Effect of electrolyte concentration on MRR at different values of voltage is shown in fig. 3.2. MRR increases with an increase in electrolyte concentration upto a certain

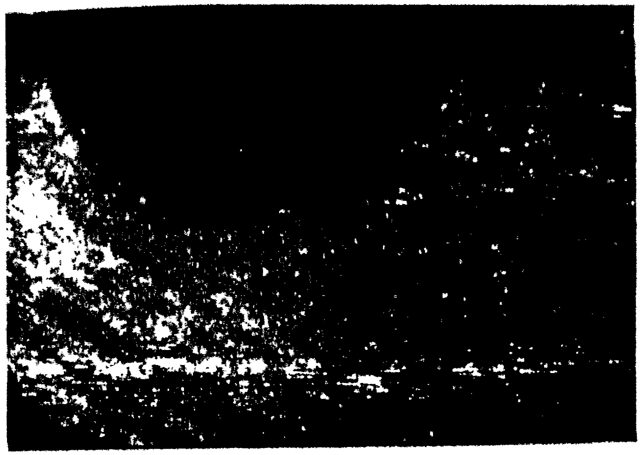

(a) Gl-ep composite
Voltage = 70 volts
Concentration = 20%
Magnification = 50X

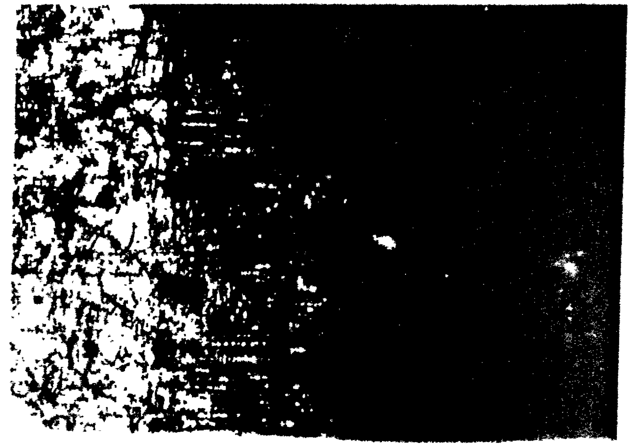

(b) Gl-ep composite
Voltage = 70 volts
Concentration = 10%
Magnification = 100X

Photograph No. 3.3 Micro-cracks

value i.e. 15% concentration, and then decreases. This is due to the fact that the specific conductance of NaOH solution increases upto 15% concentration, after which it starts decreasing. This can be observed in Fig. 2.3 and Table 2.1. An increase in specific conductance means an increased electrolyte conductivity and consequently more electrolytic current. The process of electrolysis is accelerated by an increase in the electrolytic current. This results in a greater rate of evolution of hydrogen gas bubbles at the Cahhode surface. Since, the sparking occurs across the bubble, an increased rate of H_2 gas bubbles formation implies an enhanced rate of sparking and hence higher MRR. Therefore, MRR is found to increase with increasing specific conductance and then decreases with decreasing conductance.

3.2.2 Average Diametral Overcut

Overcut was measured at various locations and then average was calculated. The dependence of the average diametral overcut (as shown in Fig. 2.3) on voltage is shown in fig. 3.3. During machining, work material is removed simultaneously by all the sides of the tool. A model in Fig. 3.9, shows the discharge through a bubble and its rupture. With an increase in voltage, the current density inceeases producing large amount of H_2 gas bubbles. So sparking rate increases resulting in wider cuts. This can be clearly seen in photograph No. 3.4. More irregular cuts

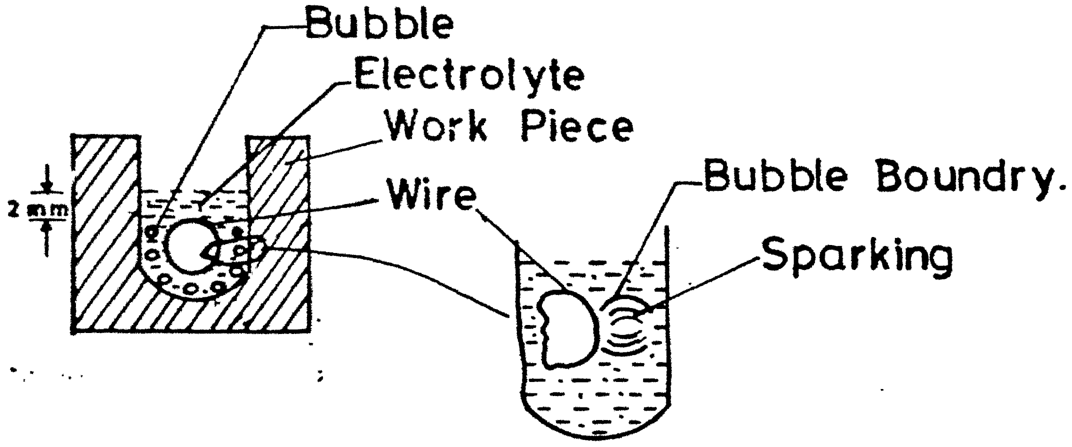

Fig. 3.9 A Model Showing the Discharge Through Bubble.

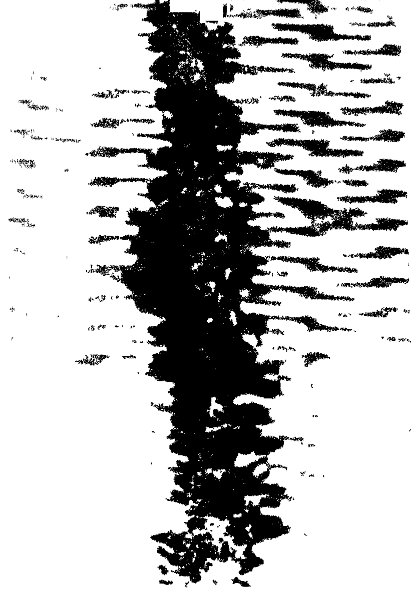

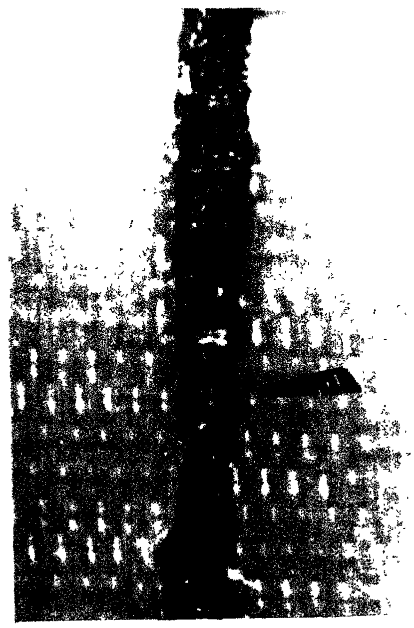

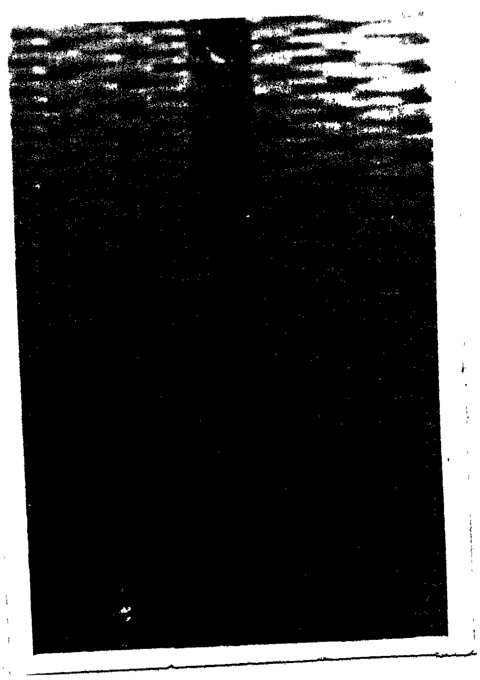

Gl- Ep COMPOSITE

VOLTAGE= 75V

CONCENTRATION= 15%.

MAGNIFICATION= 50x

FIG 3.4 (a) IRREGULAR CUT AT HIGER VOLTAGES

can be observed at higher voltages in the same photograph. The reason can be explained as follows. At higher voltages, some of the large sized bubbles are also discharge because of high potential gradient. Discharging and bursting of the bubbles of various sizes lead to highly irregular cut. Improvement in groove shape can be observed in Photograph No. 3.5 when moving wire is used instead of stationary tool.

The effect of concentration on average diametral overcut is shown in fig. 3.4. Similar to MRR, Average diametral overcut also increases upto 15%. Concentration of NaOH and then decreases. Since current density increases upto 15% concentration, after which it decreases. Effect of electrolyte concentration on overcut can be seen in photograph No. 3.6.

3.2.3 Tool Wear Rate (TWR)

TWR is defined as the reduction in weight of the tool during machining divided by the machining time.

Figures 3.5 and 3.6 show the effect of voltage and concentration on TWR, respectively. TWR is observed to increase with an increase in voltage. Similar to MRR, TWR also increases upto 15% concentration of NaOH, after which it decreases. This is similar to the dependence of MRR on these two factors and the same reasoning, as given in section 3.2.1. ~~and applies~~ applies here also. Worn out tools can be seen in Photograph No. 3.7.

GA-EP COMPOSITE
VOLTAGE = 65V
MAGNIFICATION = 50X

(a) Groove obtained with stationary tool [12]

GA-EP COMPOSITE
VOLTAGE = 65V ; CONCENTRATION = 20%.
MAGNIFICATION = 50X

(b) Groove obtained with moving wire

Photograph No. 3.5 Improvement in Groove Shape when Moving Wire is used as Cathode

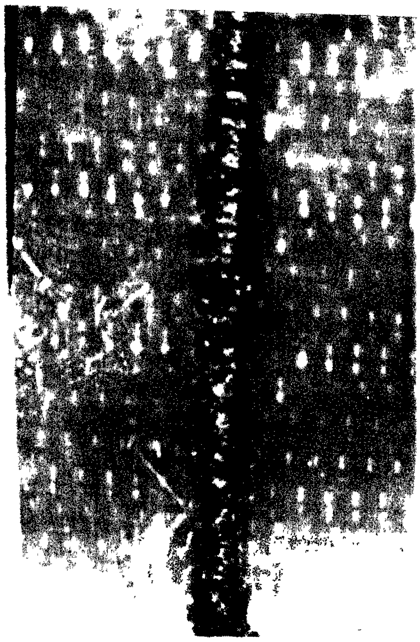

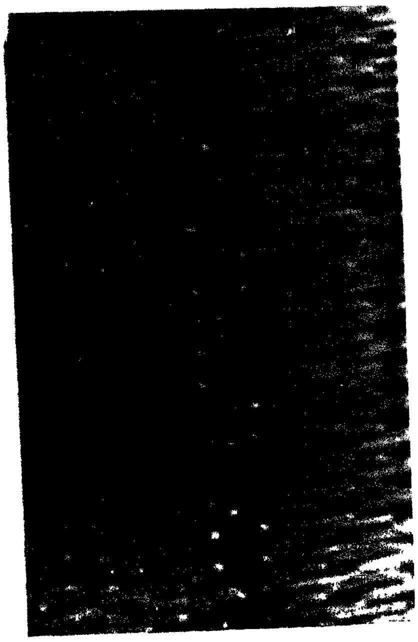

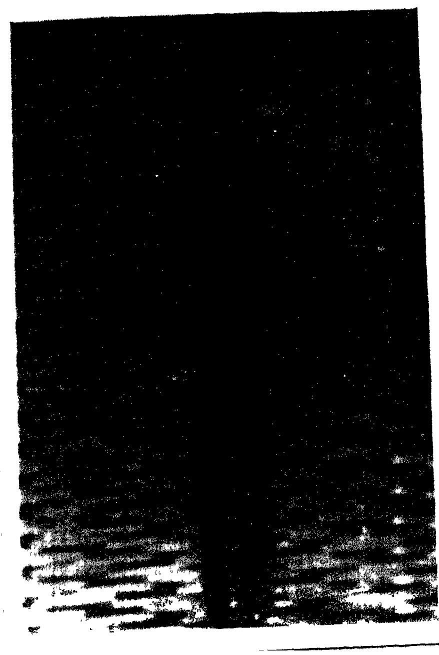

(a)

(b)

Photograph No. 3.7 Wornout Tools (a) Wornout Wire
(b) Wornout Stationary Tool [12].

3.2.4 Wire-Erosion Ratio (WER)

Wire-corrosion ratio is directly proportional to TWR and inversely proportional to MRR. Therefore, the behaviour of WRR is determined by the relative effect of a parameter on TWR and MRR.

In Fig. 3.7, WER is shown to decrease with increasing voltage. Although, both TWR and MRR increase with voltage, the effect of MRR seems to be predominant in this case and hence the decrease in WER.

Figure 3.8 shows the variation of WER with electrolyte concentration. WER is seen to decrease upto 10% concentration and then increases with increase in concentration. The effect of MRR is predominant in the beginning, after which TWR predominates.

3.3 Miscellaneous Observations

3.3.1 Voltage - Current Relationship

Figure 3.10 shows the voltage - current plot during machining. It was observed that the current suddenly drops to a lower value as soon as the sparking starts at about 50V. Afterwards i.e. at voltages higher than 50V the current flow did not remain constant but forward fluctuating.

3.3.2 Effect of Artifically Generated Bubbles on MRR and Overcut

Figure 3.11 and Figure 3.12 shows the effect of voltage

on MRR and average diameteral overcut, when the bubbles are generated in soap water and dropped on the top layer of the electrolyte. It can be seen in Fig. 3.11 that the MRR has decreased when artificial bubbles are induced. This may be due to the larger size of the induced bubbles. For the discharge to take place across these large size bubbles, high potential gradient is necessary. As soap water is used to induce bubbles, specific conductance of the electrolyte may have decreased. So intensity of sparking has reduced, hence MRR decreases.

From Fig. 3.12, it can be seen that the average diameteral overcut has decreased when artificial bubbles are induced. The above reason is applicable here also.

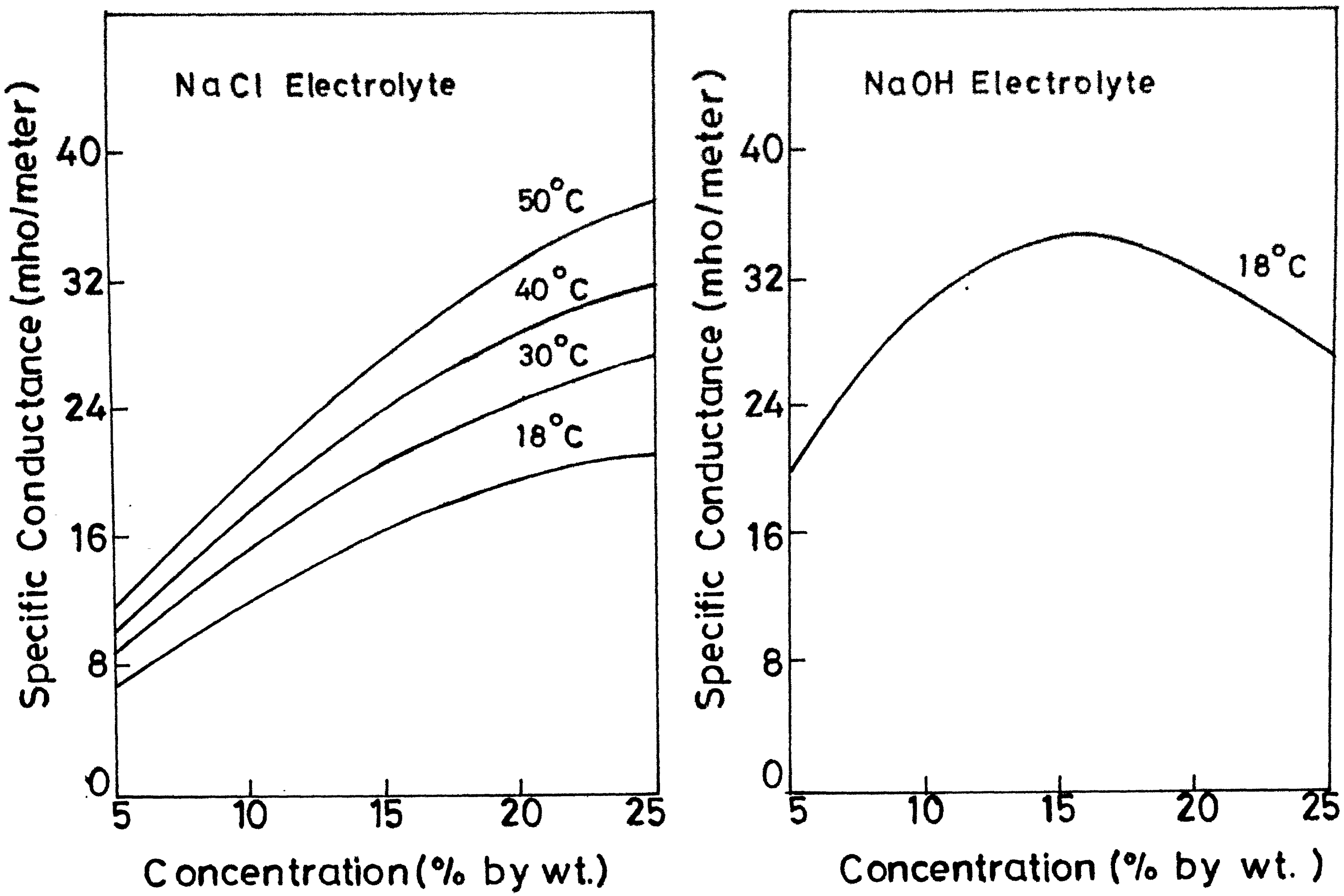

Fig. 2.3 Specific Conductance at Various Concentrations.

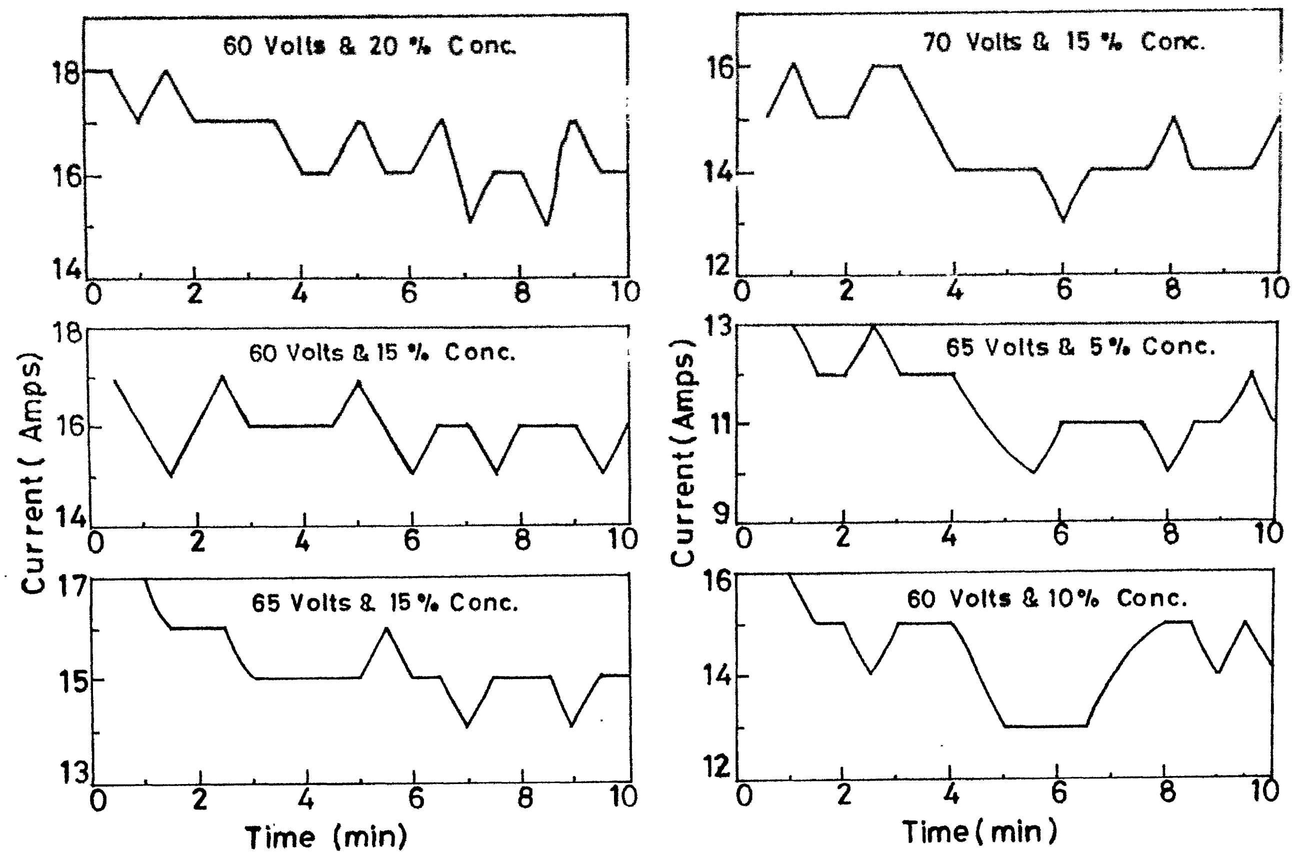

(a) Glass-Epoxy Composite

(b) Kevlar-Epoxy Composite.

Fig 2.4 History of the Current Variation During ECSM.

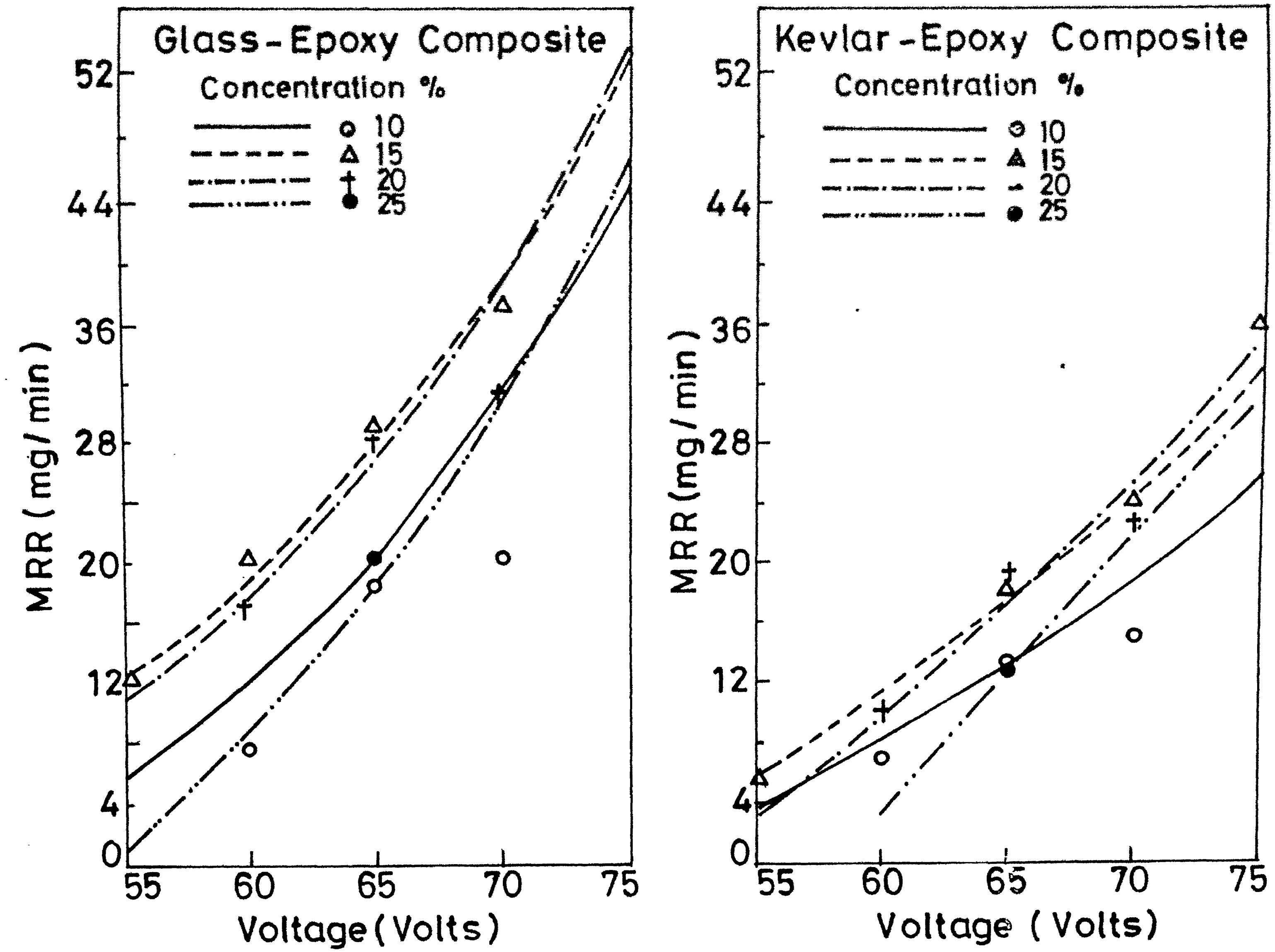

Fig. 3.1 Effect of Voltage on MRR.

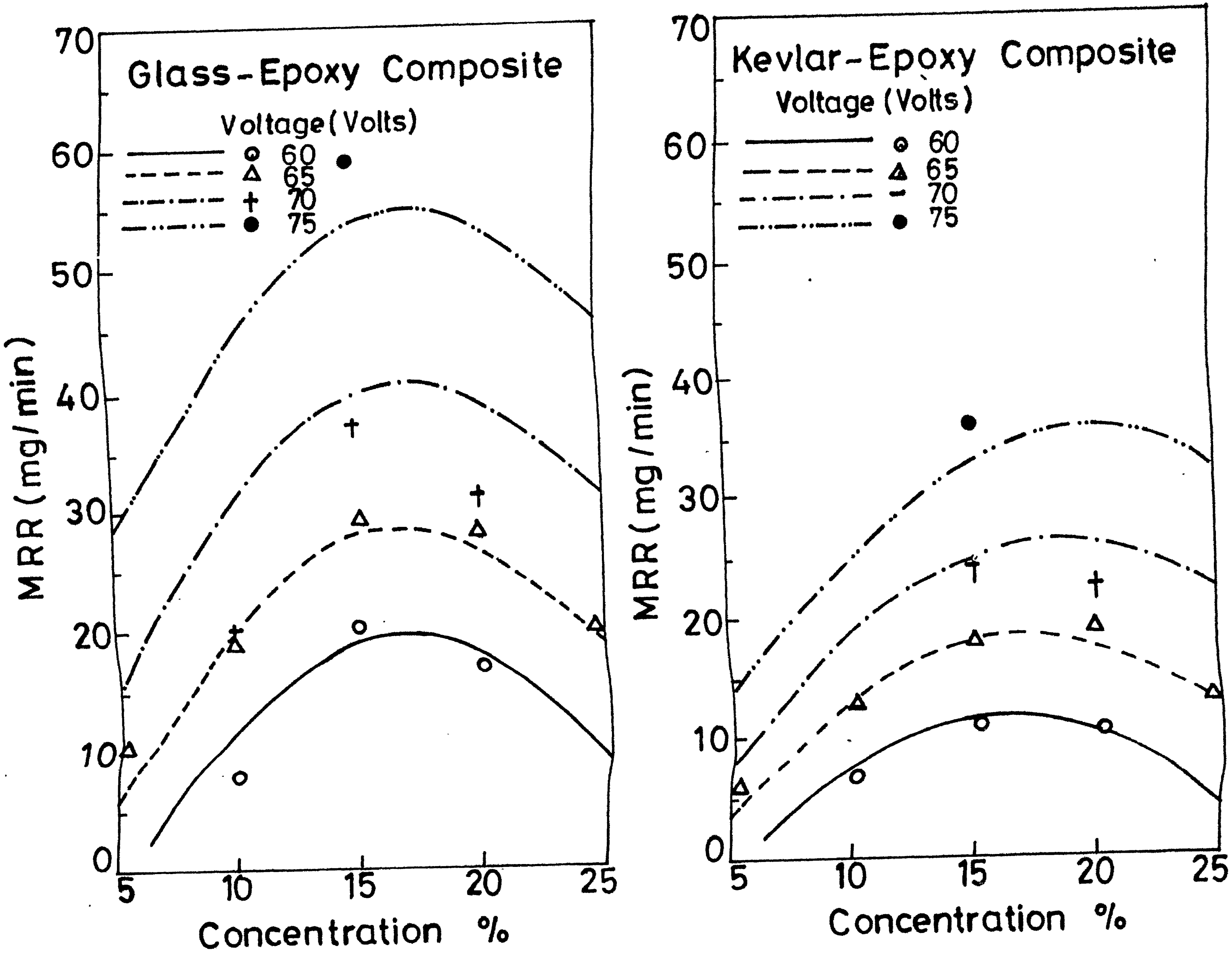

Fig 3.2 Effect of Concentration on MRR.

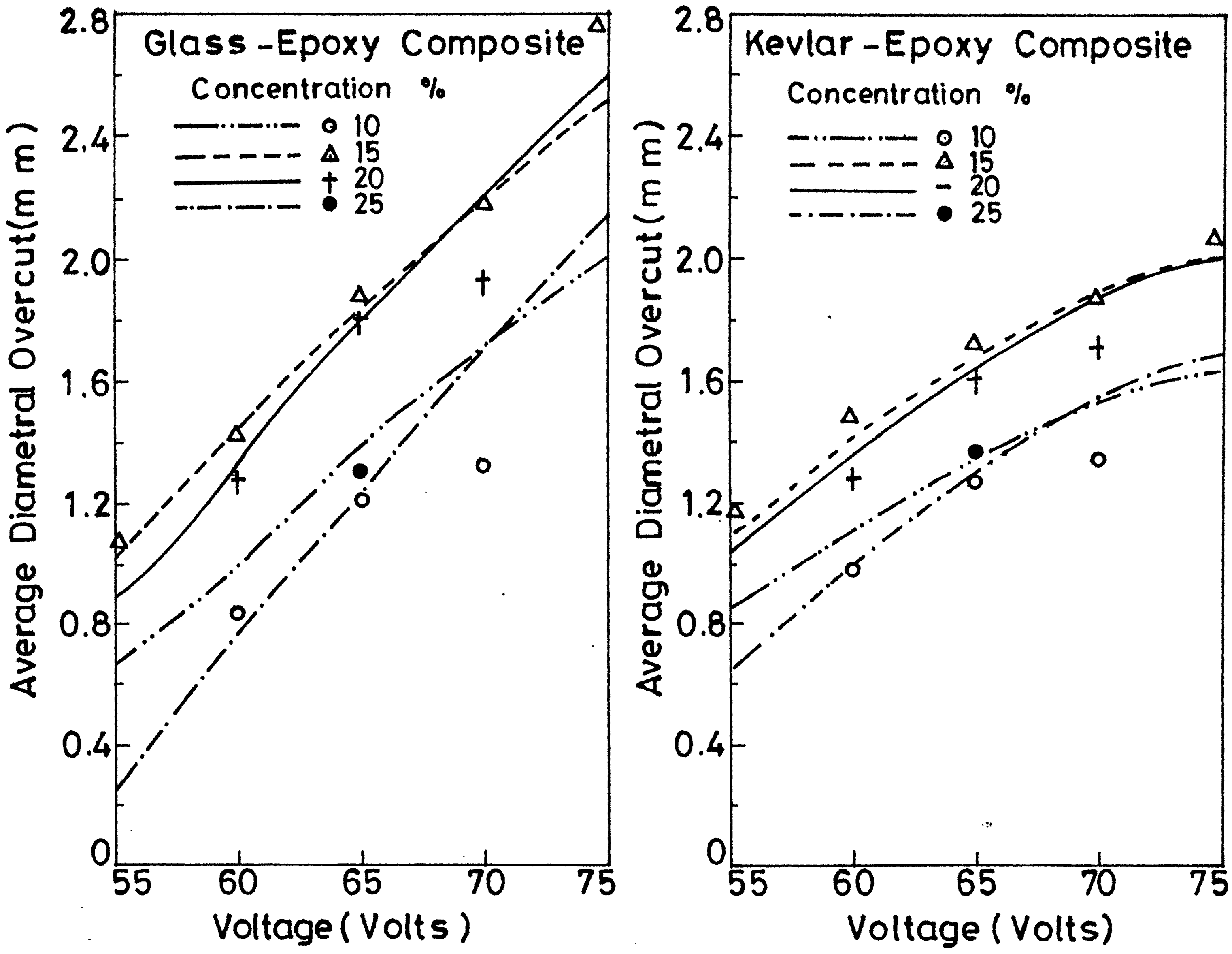

Fig. 3.3 Effect of Voltage on Average Diametral Overcut .

CENTRAL LIBRARY
I.I.T., KANPUR
No. 104234

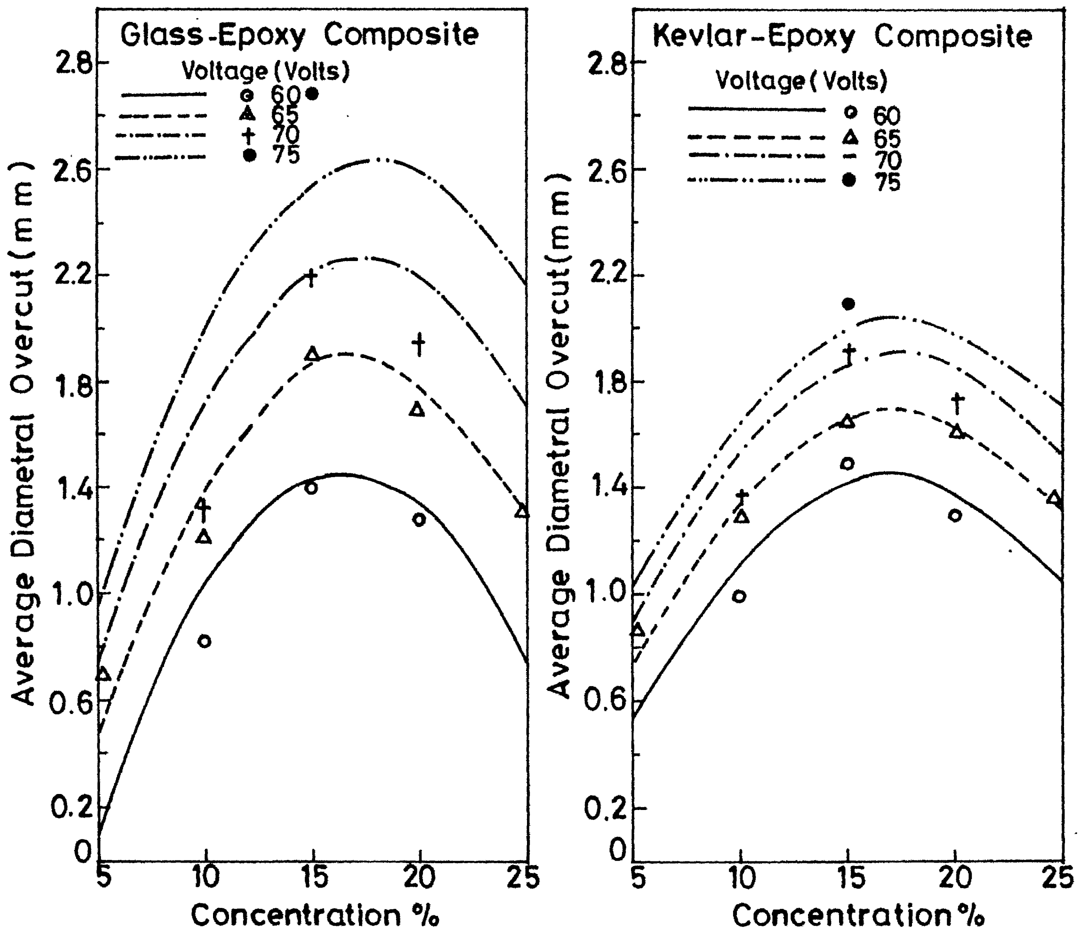

Fig. 3.4 Effect of Concentration on Average Diametral Overcut .

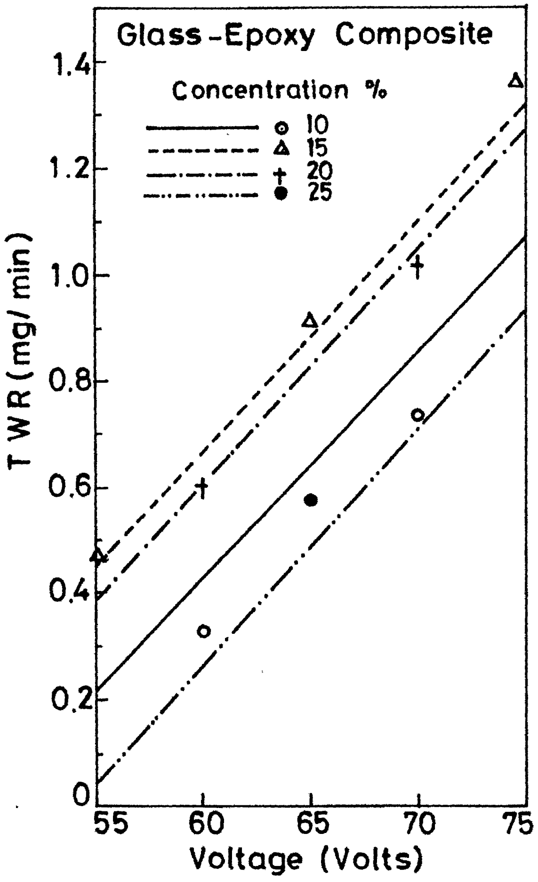

Fig. 3.5 Effect of Voltage on TWR.

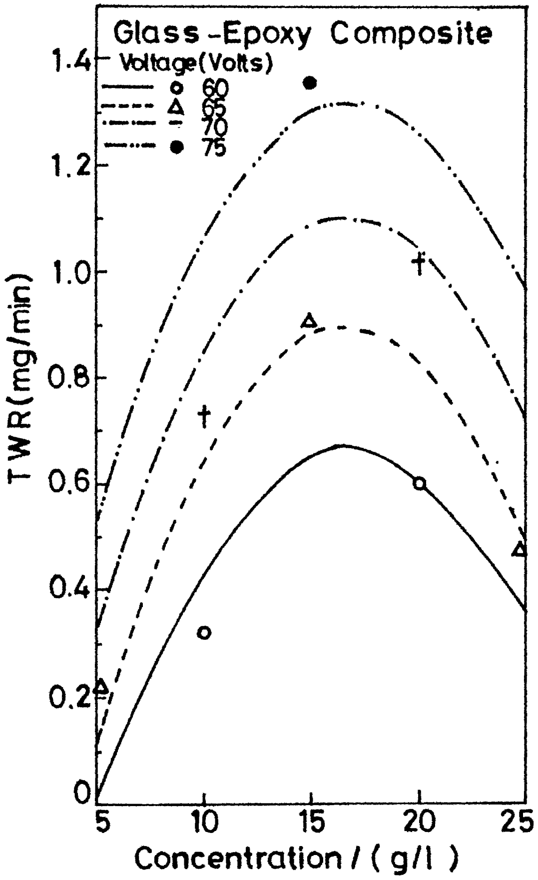

Fig.3.6 Effect of Concentration on TWR.

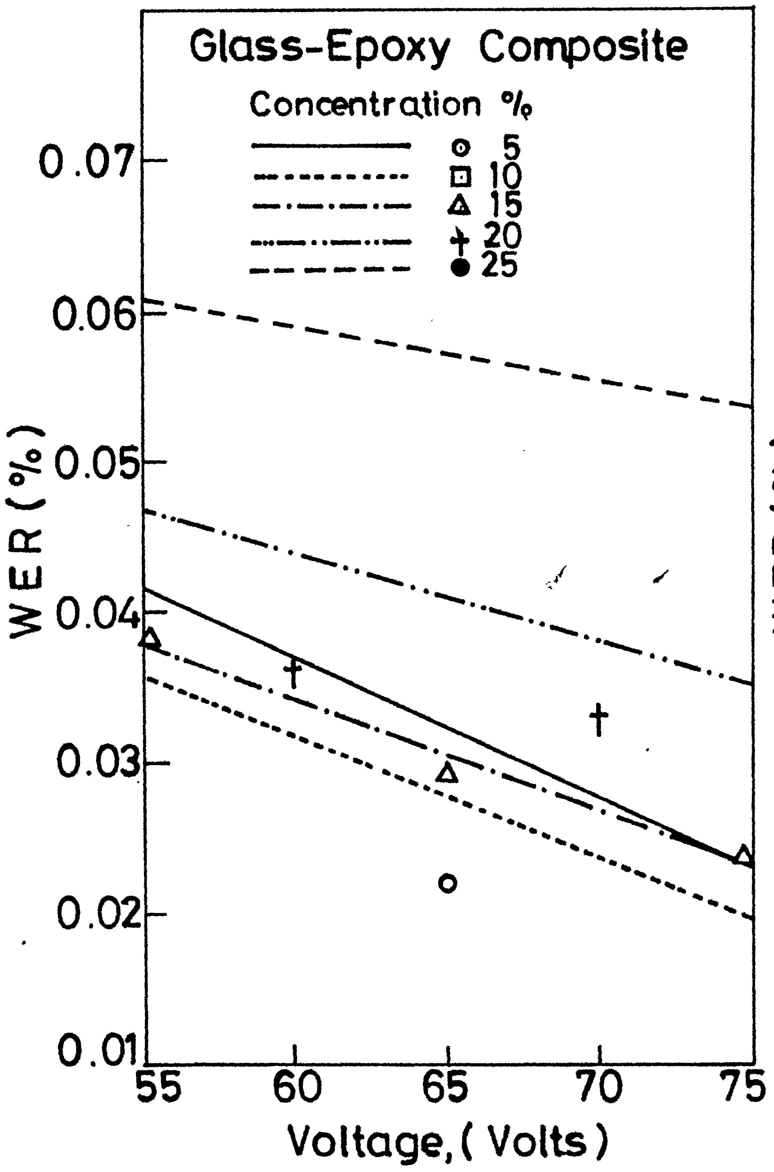

Fig. 3.7 Effect of Voltage on W E R.

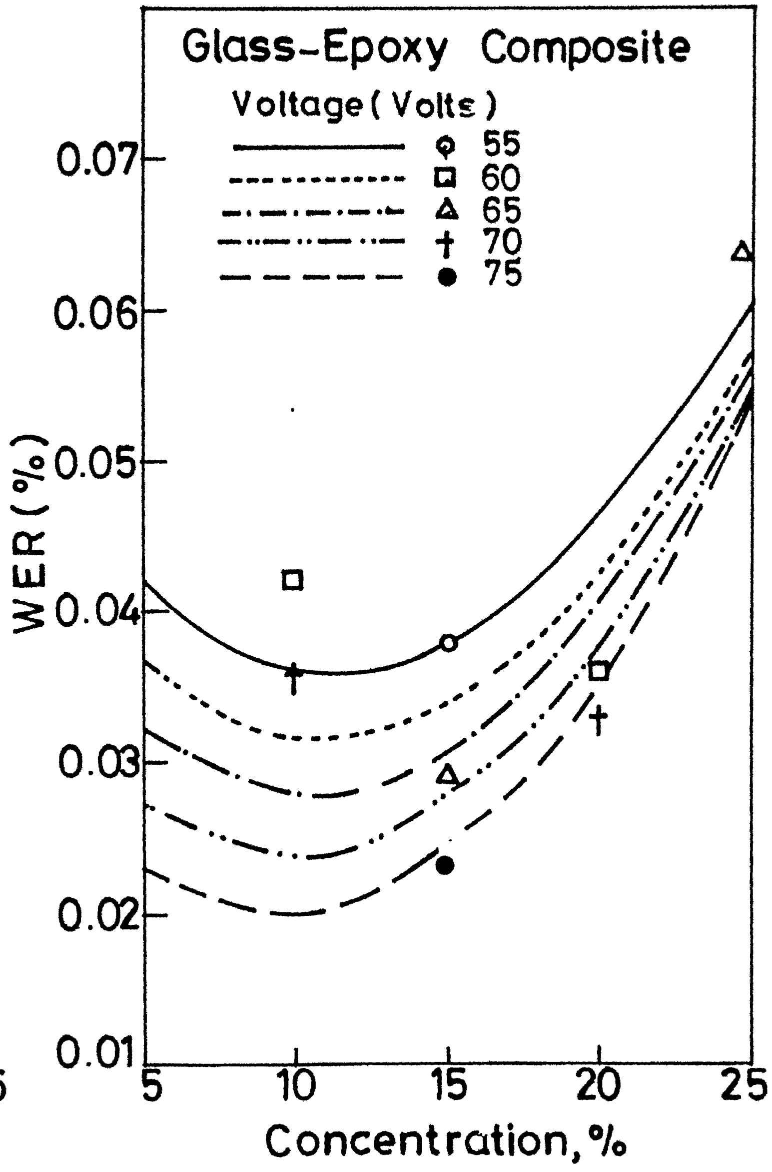

Fig. 3.8 Effect of Concentration on W E R.

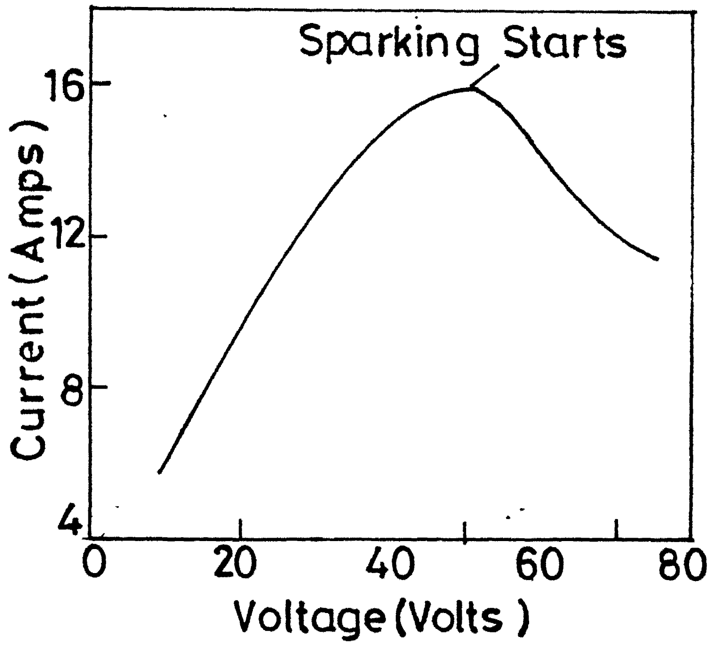

Fig 3.10 Typical Voltage-Current Plot.

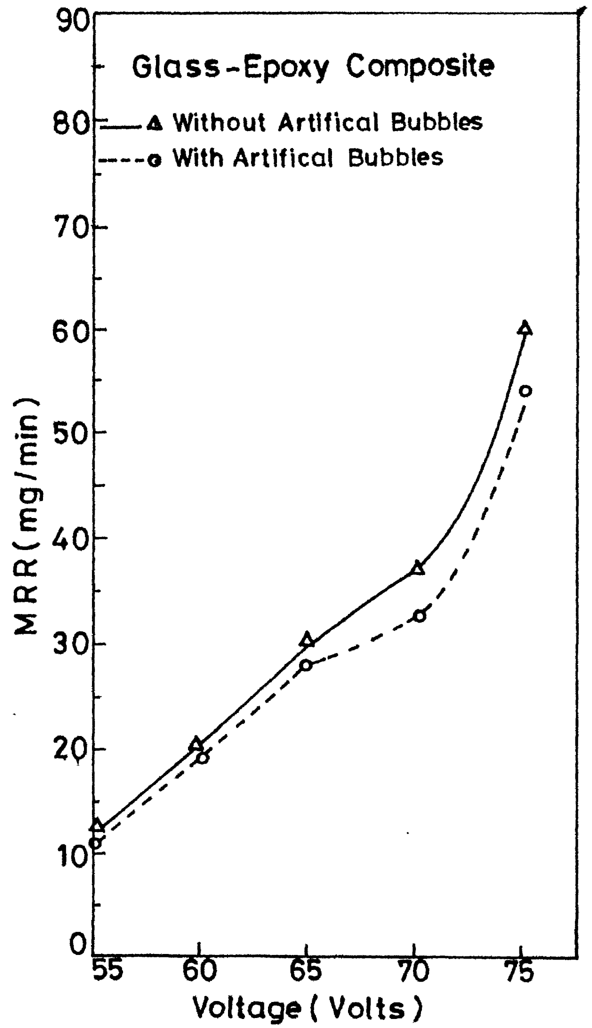

Fig. 3.11 Effect of Voltage on M R R.

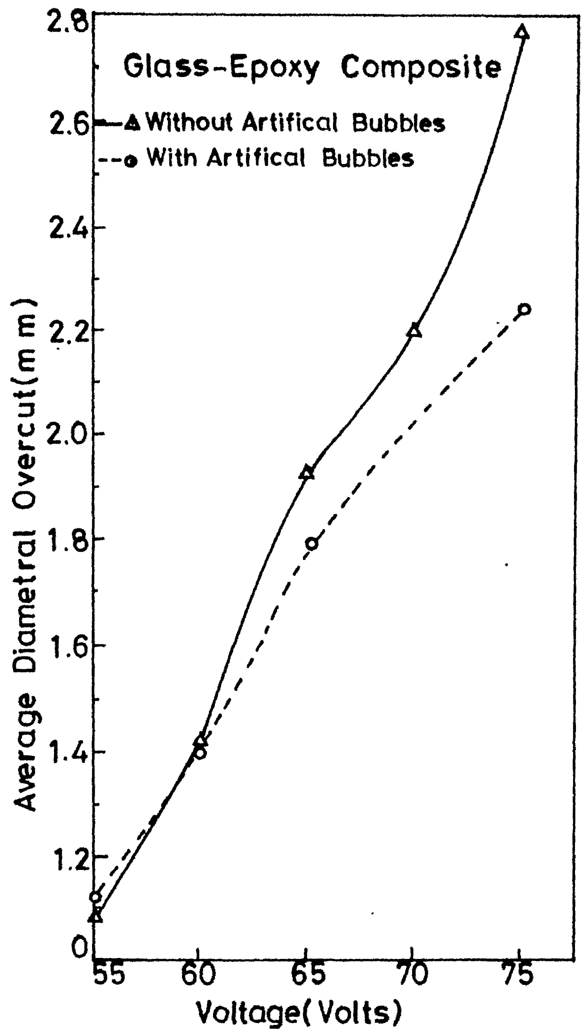

Fig. 3.12 Effect of Voltage on Overcut.

4.2 Suggestions for Future Work

Future work can be done to overcome present limitations and to develop a theoretical model for the material removal in TW/ECSM.

1. Gas could be pumped in the form of bubbles of controlled size, below the tool. This would improve the sparking and keep it alive while the electrolyte is being continuously replenished to remove any passive products if present, and to allow more hydrogen to be generated near the tool face.

2. The cathode wire could be made to vibrate or rotate, as this would remove any passive layers formed, at the tool-work interface, so that the performance of the process could be improved.

3. Pulsed d.c. could also be tried to see the effect on material removal rate and surface finish, as it would essentially mean a controlled input of energy in small units.

4. Heating of wire through an external source can be tried since it will allow more hydrogen to be generated near the surface and thus improve MRR.

5. X A suitable filter system and treatment of the electrolyte could be developed to remove the contaminating products and make the electrolyte reversable.

REFERENCES

1. Konig W., Machining of Fibre Reinforced Plastics, Annals of CIEP, Vol. 34, 1985, pp. 537-548.

2. Radhakrishnan T. and Wu S.M., On Line Hole Quality Evaluation for Drilling Composite Materials using Dynamic Data, Journal of Engineering for Industry, Vol. 103, 1981, pp. 119-125.

3. Cook, N.H., Foot, G.B., Jordan, P. and Kalyani, B.N., Experimental Studies in Electro-Machining, Journal of Engineering for Industry, Nov. 1973, pp. 945-950.

4. Schwartz, M.M., Composite Material Handbook, McGraw-Hill Book Company, 1984, Chapter 6.

5. Konig, W., New Developments in Drilling Contouring of Composites Containing Kevlar, SAMPE Fifth Technology Conference, Vol. 2, June 1984, page 16.

6. Engemann, B.K., Water Jet Cutting of Fibre Reinforced Composite Materials, Industrial and Production Engineering, Vol. 3, 1981.

7. Kumar, N.U., An Experimental Study of Electrical Machining of Non-codducting Materials, M. Tech. Thesis, IIT Kanpur, March, 1985.

8. Larsson, C.N. and Bantee E.M., Tool Damage by Sparking in ECM, IMTDR, 1977, p. 499.

9. Loutrel S.P. and Cook N.H., High Rate Electrochemical Machining, Journal of Engineering for Industry, Nov. 1973.

10. Khayry A.B.M. and McGeough J.A., Modelling of Electrochemical Arc Machining by Use of Dynamic Data Systems.

11. McGeough, J.A. and Crichton I.M., Studies of the Discharge Mechanisms in Electrochemical Arc Machining, Journal of Applied Electrochemistry, Vol. 15, 1985, pp. 113-115.

12. Sanjiv Tandon, Machining of Composites-A New Approach, M.Tech. Thesis, IIT Kanpur, July, 1987.

13. H. El-Hofy, J.A. McGeough, Evolution of an Apparatus for Electrochemical Arc Wire,Machining, Journal of Engineering for Industry, May 1988, Vol. 110, p. 119.

14. Gary F. Bendict, Non-Traditional Manufacturing Processes, Marcel Dekker, Inc., 1987.

15. Dobos, Electrochemical Data, Elsevier Scientific Publishing Company, 1975.

16. Langes Handbook of Chemistry, 10th ed., McGraw-Hill Book Company, 1961.

17. Aggarwal B.D. and Broutman L.J., Analysis and Performance of Fibre Composites, ~~Gailey~~ WILEY Interscience Publication, 1980.

18. Cochrain G.W. and Vox M.G., Experimental Designs, Asia Publishing House, 1977.

19. Adler Yop. Markove V. and Granousky Yu N., The Design of Experiments to find Optimal Conditions, Mirpublishers, Moscow, 1975.

20. Jain, V.K. and Pandey, P.C., Computer Aided Analysis of ECBD Process, Proc. of the 23rd IMT~~P~~DR Conference, 1982, pp. 257-264.

Table 2.1 : Electrical Conductivity of NaCl and NaOH Solutions

% by weight	NaCl conductivity mho/cms x 10^4	NaOH conductivity mho/cms x 10^4
5	671	2060
10	1211	3093
15	1642	3490
20	1957	3284
25	2135	2717

Table 2.2 : Kevlar Fabric Specifications

Product - Dupont Co., USA

Category - Kevlar - 49 fabrics

C.S.style - 343

Former Dupont style-143

Weight (per unit area of fabric), g/m^2 - 190

Tensile strength, N/m

Warp - 255700

Fill - 28700

Count (Number of ~~Yorn~~ Yarn/in ~~in~~ warp x fill)

- 100x20

Yarn ~~dimer~~ denier (weight in g. of 30,000 ft long yarn)

Warp - 380

Fill - 195

Weave - Crow foot

~~Finger~~ Finish - CS-805

Fiber properties:

Specific gravity = 1.44

Decomposition temp = 500°C

Table 2.3 : Epoxy Specifications

Product	-	CIBA GEIGY INDIA LTD.
Category; Resin	-	Araldite LY556
Hardner	-	Hardner HY951
		(10% of Araldite by wt.)
Mixing	-	At room temperature
Viscosity, Cp	-	5000-8000
Pot life,hr	-	0.5 - 1.00
Specific gravity	-	1.2 - 1.3
Tensile strength,Mpa	-	55-130
Tensile modulus,MPa	-	2800-4200
Poisson's ratio	-	0.20 - 0.33
Flexural strength MPa	-	125
Decomposition temp^{o}C	-	270-280

Table 2.4 : Epoxy Curing Chart

Curing Temp (^{o}C)	Curing Time
20	14-24 hr
50	5-7 hr
80	1-2 hr
100	15-30 min
140	5-10 min

APPENDIX A

In this appendix results of glass-epoxy and Kevlar-epoxy composites machining are tabulated. The experiments were performed according to "design of experiments" concept. Different combinations of independent parameters, i.e. voltage and concentration of the electrolyte and the responses obtained at each such combination are recorded in Tables 2.6 and 2.8. Four additional experiments were performed to check the validity of the models obtained from the above mentioned responses. The results of these experiments are presented in Tables 2.7 and 2.9.

Table 2.6 : Glass-epoxy Composite Machining

Sl. No.	Voltage (volts)	Concentration (% by wt.)	MRR (mg/min)	Average diametral overcut (mm)	TWR mg/min	WER (%)
1	60	10	7.521	0.819	0.319	0.0424
2	70	10	20.128	1.3065	0.726	0.0361
3	60	20	16.706	1.2651	0.603	0.0361
4	70	20	31.320	1.9437	1.024	0.0327
5	55	15	12.012	1.062	0.458	0.0381
6	75	15	59.980	2.772	1.362	0.0227
7	65	5	9.526	0.6415	0.207	0.0217
8	65	25	20.248	1.3024	0.471	0.0643
9	65	15	31.412	1.918	0.913	0.0291
10	65	15	31.741	1.933	-	
11	65	15	29.887	1.879	-	
12	65	15	29.153	1.982	-	
13	65	15	30.520	1.995	-	

Table 2.8 : Kevlar-epoxy Composite Machining

Sl.No.	Voltage (volts)	Concentration (% by wt.)	MRR (mg/min)	Avarage diametral overcut (mm)
1	60	10	6.501	0.982
2	70	10	13.823	1.346
3	60	20	10.146	1.281
4	70	20	22.608	1.719
5	55	15	5.233	1.1634
6	75	15	36.117	2.087
7	65	5	5.710	0.843
8	65	25	12.508	1.361
9	65	15	18.652	1.731
10	65	15	17.901	1.826
11	65	15	19.058	1.714
12	65	15	18.837	1.781
13	65	15	18.261	1.638

Table 2.7 : Additional Experiments for Gl-Ep Composite

Sl.No.	Voltage (volts)	Concentration (% by wt)	MRR (mg/min)	Average diametral overcut (min)
1	65	10	18.462	1.1993
2	60	15	20.014	1.4116
3	70	15	37.237	2.1862
4	65	20	28.351	1.6871

Table 2.9 : Additional Experiments for KV/Ep Composite

1	2	3	4	5
1	65	10	12.683	1.269
2	60	15	10.143	1.483
3	70	15	24.310	1.891
4	65	20	18.916	1.614

Table 2.10 : Values of Constants of Response Surface Model for Different Factors

P Surfaces	MRR		Overcut		TWR (Gl-ep)	WER (Gl-ep)
	Gl-ep	Kv-ep	Gl-ep	Kv-ep		
B_o	28.03	17.59	1.845	1.67	0.885	0.031
B_1	10.26	6.79	0.382	0.22	0.219	-0.0033
B_2	3.35	2.17	0.200	0.14	0.092	0.0063
B_{11}	1.21	0.47	-0.0132	-0.032	-0.0024	0.00017
B_{22}	-4.07	-2.42	-0.249	-0.162	-0.145	0.0033
B_{12}	0.502	1.29	0.047	0.018	0.0034	0.00072

APPENDIX B

Shadow graphs of the machined profile were taken at a magnification of 20X. These were then used to obtain the average diametral overcut produced during TW/ECSM of composites. Some of the shadow graphs of TW/ECSM of Kevlar-epoxy composite are giveb in Fig.B-1 while in figure B-2 shadow graphs of groove shapes in both glass-epoxy and Kevlar-epoxy composite are given. Figure B-1 shows how the average diametral overcut was measured.

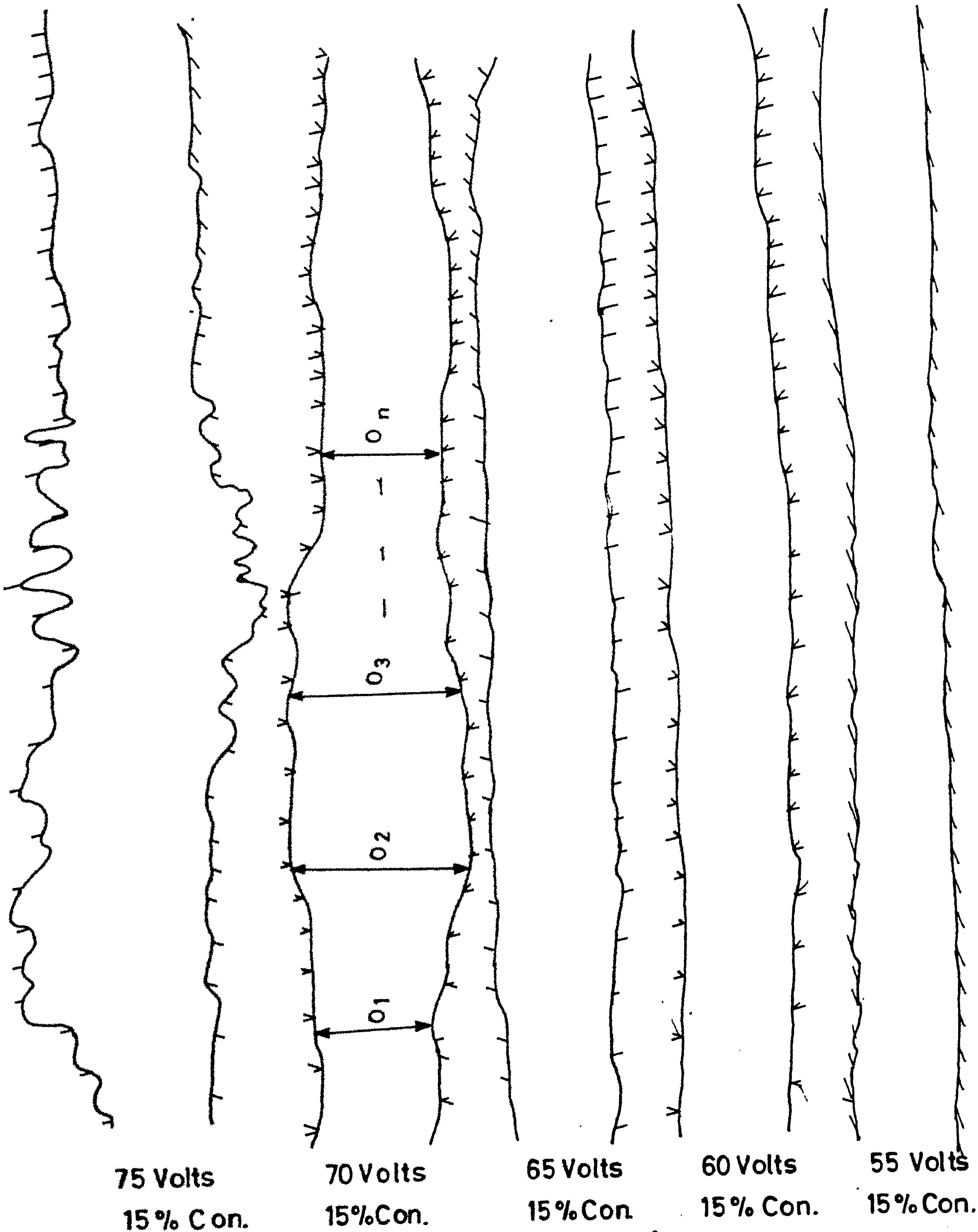

Average Diametral Overcut, $O_t = \frac{\sum_{i=1}^{n} O_i}{n} - d$

Where, O_i = Overcut at One Position
n = No. of Positions
d = Dia. of Wire

Fig. B-1 Shadowgraphs of Kevlar-Epoxy Composite Cutting.

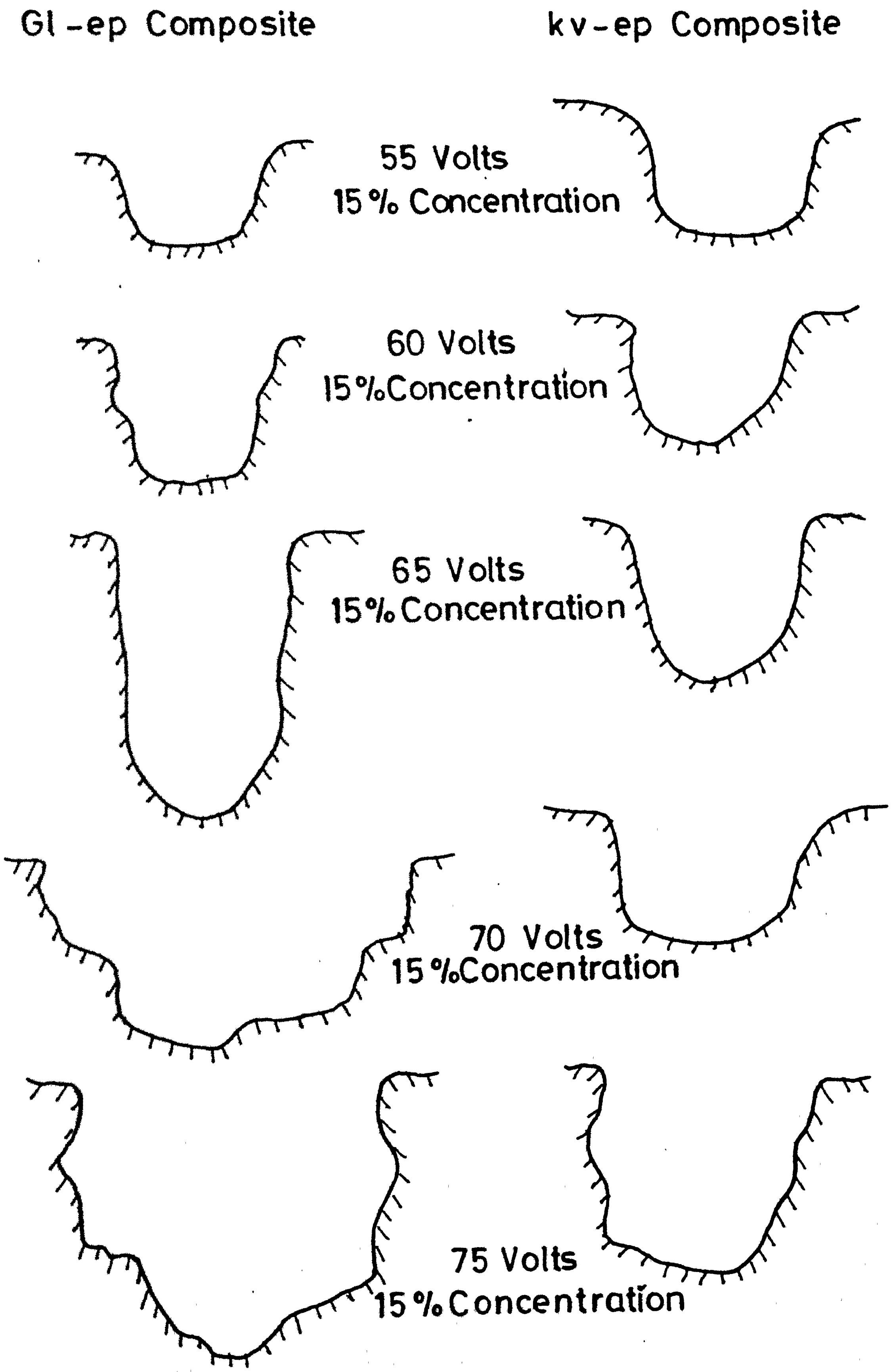

Fig B-2 Shadowgraphs of the Grooves.

104234

Th
620.118
R18a

104234

Date Slip

This book is to be returned on the date last stamped.

ME-1988-M-RAO-APP